Journal of Visualized Experiments

Quantitative analysis of cellular composition in advanced atherosclerotic lesions of smooth muscle cell lineage tracing mice

--Manuscript Draft--

Article Type:	Invited Methods Article - JoVE Produced Video
Manuscript Number:	JoVE59139R2
Full Title:	Quantitative analysis of cellular composition in advanced atherosclerotic lesions of smooth muscle cell lineage tracing mice
Keywords:	Atherosclerosis, atherosclerotic lesion, brachiocephalic artery, tissue preparation and sectioning, immunohistochemistry, immunofluorescence, confocal microscopy
Corresponding Author:	Delphine Gomez University of Pittsburgh Pittsburgh, UNITED STATES
Corresponding Author's Institution:	University of Pittsburgh
Corresponding Author E-Mail:	GOMEZD@pitt.edu
Order of Authors:	Sidney Mahan
	Mingjun Liu
	Richard A. Baylis
	Delphine Gomez
Additional Information:	
Question	**Response**
Please indicate whether this article will be Standard Access or Open Access.	Standard Access (US$2,400)
Please indicate the **city, state/province, and country** where this article will be **filmed**. Please do not use abbreviations.	Pittsburgh, PA, USA

University of Pittsburgh
School of Medicine
Vascular Medicine Institute

Delphine Gomez, PhD
Assistant Professor of Medicine
University of Pittsburgh
Department of Medicine, Division of Cardiology
200 Lothrop Street
Biomedical Science Tower, room 1723
Pittsburgh PA 15261
gomezd@pitt.edu
412-383-3269

Wednesday, November 21, 2018

Dear Phillip Steindel,

We are pleased to submit a revised version of the manuscript JoVE59139, entitled " Quantitative analysis of cellular composition in advanced atherosclerotic lesions of smooth muscle cell lineage tracing mice" for consideration for publication in JoVE.

We thank the Editor and the four Reviewers for their constructive comments. We have carefully edited the manuscript to address the majority of the Reviewer's concerns and comments. We have made significant modifications of the figures to increase the quality of the pictures.

We opted to develop a new protocol to perform single-cell counting using ImageJ, free software developed by the NIH and accessible to everybody. As such, our protocol can be performed by all investigator independently of the brand of confocal microscope used.

We illustrated single cell counting with ImageJ in Figure 5 by taking screen captures. Then, we gave two examples of single cell counting analyses with matching immunofluorescent staining: SMC and macrophage quantification in the fibrous cap area at two locations of the brachiocephalic artery in Figure 6 and the quantification of RUNX2+ chondrogenic cells in Figure 7.

We feel these modifications have increased the overall quality of the manuscript.

We are looking forward to hearing from the JoVE editorial team.

Sincerely,

Delphine Gomez

TITLE:

Quantitative Analysis of Cellular Composition in Advanced Atherosclerotic Lesions of Smooth Muscle Cell Lineage-Tracing Mice

AUTHORS AND AFFILIATIONS:

Sidney Mahan[1], Mingjun Liu[1], Richard A. Baylis[2,3], Delphine Gomez[1,4]

[1]Heart, Lung, Blood and Vascular Medicine Institute, University of Pittsburgh
[2]Robert M. Berne Cardiovascular Research Center, University of Virginia
[3]Department of Biochemistry and Molecular Genetics, University of Virginia
[4]Division of Cardiology, University of Pittsburgh School of Medicine; Pittsburgh

Corresponding Author:
Delphine Gomez (gomezd@pitt.edu)
Phone: 412-383-3269

Email Addresses of Co-Authors:
Sidney Mahan (sam395@pitt.edu)
Mingjun Liu (mil128@pitt.edu)
Richard A. Baylis (rab5uh@virginia.edu)

KEYWORDS:
atherosclerosis, atherosclerotic lesion, brachiocephalic artery, tissue preparation and sectioning, immunohistochemistry, immunofluorescence, confocal microscopy

SUMMARY:

We propose a standardized protocol to characterize the cellular composition of late-stage murine atherosclerotic lesions including systematic methods of animal dissection, tissue embedding, sectioning, staining, and analysis of brachiocephalic arteries from atheroprone smooth muscle cell lineage tracing mice.

ABSTRACT:

Atherosclerosis remains the leading cause of death worldwide and, despite countless preclinical studies describing promising therapeutic targets, novel interventions have remained elusive. This is likely due, in part, to a reliance on preclinical prevention models investigating the effects of genetic manipulations or pharmacological treatments on atherosclerosis development rather than the established disease. Also, results of these studies are often confounding because of the use of superficial lesion analyses and a lack of characterization of lesion cell populations. To help overcome these translational hurdles, we propose an increased reliance on intervention models that employ investigation of changes in cellular composition at a single cell level by immunofluorescent staining and confocal microscopy. To this end, we describe a protocol for

testing a putative therapeutic agent in a murine intervention model including a systematic approach for animal dissection, embedding, sectioning, staining, and quantification of brachiocephalic artery lesions. In addition, due to the phenotypic diversity of cells within late-stage atherosclerotic lesions, we describe the importance of using cell-specific, inducible lineage tracing mouse systems and how this can be leveraged for unbiased characterization of atherosclerotic lesion cell populations. Together, these strategies may assist vascular biologists to more accurately model therapeutic interventions and analyze atherosclerotic disease and will hopefully translate into a higher rate of success in clinical trials.

INTRODUCTION:

Atherosclerosis is the leading cause of morbidity and mortality worldwide underlying the majority of coronary artery disease, peripheral artery diseases, and stroke. Late-stage coronary atherosclerosis can lead to severe complications including myocardial infraction accounting for nearly 16% of world population mortality[1,2]. Due to its devastating impact on public health, substantial effort has been made to decipher the mechanisms driving atherosclerosis progression, as well as to develop novel therapeutic strategies. Yet, the Likelihood of Approval (LOA) rate of clinical trials for cardiovascular disease is among the lowest when compared with other clinical fields (only 8.7% for phase I)[3]. This can be explained in part by many barriers that atherosclerosis poses to efficient drug development including its nearly ubiquitous nature, clinically-silent progression, and significant disease heterogeneity. Moreover, the suboptimal design of preclinical animal studies can also be accounted for the lack of success in clinical translation. Specifically, we believe it is necessary to implement intervention studies whenever possible to investigate the efficacy of therapeutic strategies. Also, there is a critical need to perform standardized procedures for lesion analyses including advanced characterization of late-stage atherosclerotic lesion cellular composition by fate mapping and phenotyping.

The vast majority of atherosclerosis studies focus on models of atherosclerosis prevention consisting of drug treatment or gene manipulation (knockout or knock-in) in healthy young mice, prior to the disease initiation and progression. These studies have uncovered a large number of genes and signaling molecules that play a role in atherosclerosis development. However, most of these targets failed to translate to efficient therapies in human. Indeed, it is difficult to extrapolate the effect a therapy has on healthy young mice to elderly patients with advanced atherosclerotic lesions. As such, the implementation of intervention studies in the preclinical experimental pipeline likely provides a more accurate depiction of the relevance and efficacy of a new therapeutic. The idea is supported by the strikingly divergent effects of inhibiting the pro-inflammatory cytokine Interleukin-1β (IL-1β) when employing a prevention[4–6] or intervention strategy[7]. Differences between prevention and intervention studies suggest that different cellular processes occur at different phases of atherosclerosis development and highlights the fact that prevention studies are likely insufficient to model the clinical scenario adequately.

The American Heart Association recently published a scientific statement detailing recommendations for proper experimental design, procedural standardization, analysis, and reporting of animal atherosclerosis studies[8]. It highlights the benefits and limitations of

predominant techniques used in the field. For example, *en face* Sudan IV staining of the aorta is often performed as a first read-out. Although *en face* Sudan IV staining of lipid deposition is a suitable method for assessment of global plaque burden, it is unable to distinguish early-stage fatty streak lesions from more advanced late-stage lesions. As such, the interpretation of *en face* staining is often ambiguous and superficial[9]. Careful analysis of tissue cross sections using the morphologic parameters vessel, lesion, and lumen size and quantification of indices of lesion stability provides a more accurate understanding of the effect of an experiment.

Finally, human histopathology studies have suggested that cellular composition is a better predictor of rupture than the lesion size itself, with lesions poor in smooth muscle cells (SMC) and rich in macrophages being more susceptible to rupture[10,11]. These observations were based on staining for markers classically used for cell identification (i.e., ACTA2 for SMC and LGALS3 or CD68 for macrophages). However, the expression of these markers is not strictly restricted to a single cell type in atherosclerotic lesions due to the plasticity of multiple lineages including SMC, endothelial cells and myeloid cells[12]. In particular, the unambiguous identification of SMC within atherosclerotic lesion was virtually impossible until the past decade because of the property of these cells to dedifferentiate and repress their lineage-specific marker genes (a process referred as phenotypic switching) in injured or diseased vessels[13]. This limitation in SMC identification has been circumvented by the development of lineage tracing[7,14–24]. It consists of permanently labelling SMC and their progeny to track their fate and phenotypic evolution during atherosclerosis progression by using a combination of the expression of Cre recombinase driven by SMC-specific promoters (i.e., *Myh11*[7,15,17-24], *Acta2*[25,26] and, *SM22*α[14,16]) and the activation of reporters (e.g., fluorescent proteins, β-galactosidase) [reviewed in Bentzon and Majesky 2018[27]]. In one of the first studies employing SMC lineage tracing outside of embryogenesis setting, Speer et al.[14] provided evidence that SMC can modulate their phenotype and transdifferentiate into chondrogenic cells during vascular calcification by using an *SM22*α Cre R26R LacZ lineage tracing model. Although these studies pioneered SMC lineage tracing, they were partially equivocal in that any given non-SMC expressing SM22α in the setting of the disease would be labeled by the reporter. This limitation has been bypassed by the development and use of tamoxifen-inducible Cre ERT/LoxP permitting a temporal control of cell labeling. Cell labeling occurs exclusively during tamoxifen delivery and will be restricted to the cell expressing the cell type-specific promoter driving Cre ERT expression at the time of tamoxifen exposure, avoiding tracing of alternative cell types activating Cre in the setting of disease progression. For lineage tracing of SMC in atherosclerosis, the tamoxifen-inducible *Myh11*-Cre/ERT2 transgene associated with fluorescent reporters (eYFP[7,15,17,18,21], mTmG[19,25], Confetti[20,22,23] for clonal expansion studies) has demonstrated a remarkable efficiency and specificity in SMC labeling and has been used to fate map SMC populations in atherosclerotic lesions in recent studies. Importantly, these studies revealed that: 1) 80% of SMC within advanced atherosclerotic lesions do not express any conventional SMC markers (ACTA2, MYH11) used in immunohistological analysis and therefore would have been misidentified without lineage tracing[17]; 2) subsets of SMC express markers of alternate cell types including macrophage markers or mesenchymal stem cell markers[16,17,19]; and 3) SMC invest and populate the atherosclerotic lesion by oligoclonal expansion and SMC clones retain plasticity to transition to phenotypically different populations[20,23]. To summarize, it is now clear that smooth muscle cells present a remarkable phenotypic diversity in atherosclerotic

lesions and can have beneficial or detrimental roles on lesion pathogenesis depending on the nature of their phenotypic transitions. These discoveries represent a remarkable new therapeutic avenue for targeting SMC athero-promoting phenotypic transitions in late-stage atherosclerosis.

Herein, we propose a standardized protocol for analyzing late-stage murine atherosclerotic lesions including systematic methods for animal dissection, embedding, sectioning, staining, and quantification of brachiocephalic artery lesions. To determine the effect of Interleukin-1β inhibition on SMC fate and phenotype, we used SMC lineage tracing ApoE$^{-/-}$ mice fed a western diet for 18 weeks before receiving weekly injections of an anti-IL1β antibody or isotype-matched IgG control.

PROTOCOL:

Animal breeding, handling and procedures were approved by the University of Virginia and the University of Pittsburgh Institutional Animal Care and Use Committee.

1. Generation of SMC lineage tracing mice

1.1. Breed *Myh11*-Cre/ERT2 males[28] (Jackson Laboratory; #019079) with R26R-EYFP females (Jackson Laboratory; #006148) to obtain *Myh11*-Cre/ERT2^{+} R26R-EYFP$^{+/+}$ males.

1.2. Breed the *Myh11*-Cre/ERT2^{+} R26R-EYFP$^{+/+}$ males with ApoE$^{-/-}$ female mice (Jackson laboratory; #002052). Cross the progeny and select by genotyping *Myh11*-Cre/ERT2^{+} R26R-EYFP$^{+/+}$ ApoE$^{-/-}$ male and R26R-EYFP$^{+/+}$ ApoE$^{-/-}$ female mice as final breeders. Clip tails and perform genotyping on littermates. All male mice should be *Myh11*-Cre/ERT2^{+} R26R-EYFP$^{+/+}$ ApoE$^{-/-}$ and can be used as experimental mice (**Figure 1A**).

NOTE: Genotyping protocols can be found on the Jackson Laboratory website. The *Myh11* Cre/ERT2 transgene is located on the Y chromosome, precluding the use of females. Other lineage tracing systems can be used, but this system is to date the most reliable lineage tracing strategy to fate map SMC in atherosclerosis.

2. Smooth muscle cell lineage-tracing mouse diet and treatments

2.1. Have male *Myh11*-Cre/ERT2^{+} R26R-EYFP$^{+/+}$ ApoE$^{-/-}$ mice receive a series of 1 mg tamoxifen injections from six to eight weeks of age to label permanently Myh11^{+} SMC with YFP and to track their fate (**Figure 1A**).

2.1.1. Heat peanut oil at 55 °C.

2.1.2. Add tamoxifen in pre-heated peanut oil to prepare a solution at 10 mg/mL and incubate at 55 °C until complete dissolution of tamoxifen.

2.1.3. Perform an intraperitoneal injection with 0.1 mL of 10 mg/mL tamoxifen solution for a series of ten injections over two weeks.

NOTE: Tamoxifen is a biohazard and must be handled with care.

2.2. Five to seven days after the last injection with tamoxifen, replace chow diet with high-fat diet (e.g., western diet; 42% kcal from fat; 0.2% total cholesterol) for a duration of 18 weeks to allow for the development of advanced atherosclerotic lesions, which consistently develops in multiple vascular beds including the aortic arch, aortic root, brachiocephalic artery and the abdominal aorta.

2.3. At 18 weeks of high-fat diet feeding, begin therapeutic intervention for the desired duration (**Figure 1B**).

NOTE: As an example, we performed weekly intraperitoneal injections with an anti-IL1β antibody or an isotype-matched IgG control between 18 and 26 weeks of high fat diet.

2.4. Remove food to fast mice for 8 to 16 h prior to tissue harvesting to perform accurate readings for plasma cholesterol and triglyceride.

3. Harvesting of the Brachiocephalic Artery (BCA)

3.1. Animal euthanasia should follow Animal Care and Use Committee (ACUC) requirements and regulations. Euthanize the experimental mice by CO_2 asphyxiation for approximatively 5 minutes and verify death by toe pinch.

3.2. Weigh the mouse and collect blood.

3.2.1. Weigh the mouse

3.2.2. Spray the ventral side of the mouse with 70% Ethanol

3.2.3. Perform cardiac puncture by inserting a 25G needle connected to a 1 mL syringe in the ventricle from the left side of the chest cavity. 0.1 to 1 mL of blood can be collected.

3.2.4. Transfer the blood to an EDTA vacuum tube by flushing the syringe and place the tube on a rocker or rotator for 10-15 min.

3.2.5. Transfer blood to a 1.5 mL tube and centrifuge for 10 minutes 250 x *g* at 4 °C. Carefully withdraw the top plasma phase with a pipette and adequate tips, and transfer to a new tube. Store at -20 °C prior to measuring cholesterol and triglycerides.

NOTE: Whole blood can be used for additional studies including blood cell counts and other blood components including cytokines or immune cell profiling.

3.3. Make an incision of approximatively 2 cm in the skin at the mid-abdomen using scissors and pull the skin to expose the abdominal cavity. Cut the peritoneum up to the sternum without damaging tissues. Make two cuts at the mid-axillary line through the thorax, being careful not to damage the heart and lungs.

3.4. Lift the sternum with tweezers and cut the diaphragm to partially expose the heart. If the heart is not easily accessible, cut away the ribcage enough to reach the right atrium.

3.5. Perfuse the mouse with a gravity perfusion system (**Figure 2A**). Install the gravity perfusion system such that the pressure of the perfusion fluid is equivalent to the average murine blood pressure (**Figure 2B**). This system allows for consistency in perfusion and both maintains the vessel morphology and flushes red blood cells.

NOTE: As reference, C57Bl6 mice have a physiologic blood pressure between 120 mmHg (average systolic blood pressure) and 70 mmHg (average diastolic blood pressure)[29,30]. Average systolic and diastolic blood pressure can vary with mouse genetic background.

3.5.1. Connect a 23 or 25G butterfly needle to the gravity perfusion system and run Phosphate-buffered Saline (PBS) through the needle to expel the air from the tubes. Insert the needle into the left ventricle and secure the needle in place. Using iris scissors, make a small incision (< 2 mm) into the right atrium or the ascending aorta.

3.5.2. Perfuse with 5 mL of PBS, then 10 mL of 4% Paraformaldehyde (PFA) solution, then 5 mL of PBS. Use both PBS and 4% PFA solution at ambient temperature.

3.5.3. Collect the tissues of interest (e.g., liver, lung, spleen) and place them in the 4% PFA solution.

3.6. Expose the BCA

3.6.1. Clean the neck area by removing the skin and salivary glands.

3.6.2. Perform one cut down the midline of the sternum through the manubrium using scissors. Be careful that the scissors stay close to the back of the sternum to avoid damaging the vasculature located closely below the sternum. Pull both sides of the ribcage with forceps to fully open the chest cavity. Carotids should be partially visible.

3.6.3. Clean up by pulling muscles and connective tissue and removing fat with fine tweezers until the right carotid, the brachiocephalic artery the subclavian bifurcation and the aortic arch are cleaned and isolated of surrounding connective tissue and fat (**Figure 2C**).

3.7. Remove the BCA

3.7.1. Using forceps, grab the right carotid below its bifurcation and make an initial cut above the forceps (**Figure 2D**).

3.7.2. Still holding the carotid, make a second cut through the subclavian artery. The final two cuts are through the aortic arch, on either side of the brachiocephalic artery (**Figure 2D**).

3.7.3. Collect other vascular tissues of interest (e.g., abdominal aorta, superior part of the heart containing the aortic root).

3.7.4. Place the BCA and other tissues in 4% PFA solution overnight at room temperature.

NOTE: The fixation time should be kept consistent throughout the study.

4. Tissue processing and sectioning

4.1. Remove the tissue from 4% PFA and place in a labeled tissue cassette (**Figure 3A**). Use foam pads in the cassette to ensure the tissue retain its orientation and remains in the cassette through the processing step (**Figure 3B**). Close the cassettes and immerse in 70% ethanol until tissue processing (24 to 72h).

4.1.1. Process BCA and other tissues collected for histological and immunofluorescent staining as follows (example of routine overnight procedure using a processor with vacuum penetration): 10% neutral buffered formalin for 30 min at ambient temperature (2x), 75% ethanol for 60 min at 30 °C (1x), 90% ethanol for 60 min at 30 °C (1x), 95% ethanol for 60 min at 30 °C (1x), 100% ethanol for 60 min at 30 °C (3x), xylene for 60 min at 30 °C (3x), and paraffin wax for 80 min at 62 °C (3x).

4.2. Embed BCA vertically, with the aortic arch closest to the block face (**Figure 3C**).

4.3. Cut through the paraffin block on a rotary microtome (10 µm thickness) until reaching the embedded tissue.

4.4. Once the tissue is visible, examine a section under a microscope to determine position. If the aortic arch is still visible, remove up to ten 10 µm sections at a time, examining a section at each interval.

4.5. When the aortic arch has been sectioned through and the brachiocephalic artery is visible, adjust the orientation of the block to position the tissue completely perpendicular to the microtome blade.

4.6. Cut the BCA at a section thickness of 10 µm. At that point, all sections are collected serially with three sections per slide. Collect until reaching the subclavian bifurcation (**Figure 3D**).

NOTE: It is important to cut the BCA at a section thickness of 10 µm for subsequent z-stack

confocal image acquisition and single cell counting. This thickness will allow the rigorous and non-cofounding assessment of the association between a single nucleus and cytoplasmic or membrane staining though the depth of the cross section.

5. Immunofluorescent staining

NOTE: A complete characterization of atherosclerotic lesions includes assessment of morphological parameters and indices of plaque stability or instability and cellular composition that will not be the focus of the present protocol. Lesion morphology, collagen content, and intraplaque hemorrhage can be analyzed by Movat[7,17], PicroSirius Red [7,31], Ter119 staining [7,18], respectively. Here, we will describe the protocol for analyzing the cellular composition of lesions.

5.1. Incubate the slides in the following solutions at room temperature under a chemical hood: xylene for 5 min (2x), 100% ethanol for 5 min (2x), 95% ethanol for 5 min (2x), 70% ethanol for 5 min (2x), and deionized H2O (diH2O) for 5 min (2x).

5.2. Incubate slides in antigen retrieval solution according to manufacturer's instruction.

5.2.1. With citric acid based antigen unmasking solution (see **Table of Materials**), dilute 3 mL of solution in 320 mL of diH2O. Place the slides in a staining reservoir and fill to the top with the prepared antigen retrieval solution.

5.2.2. Fill any empty slots in the slide rack with blank slides to ensure even heating. Cover the container with a lid to allow the antigen retrieval solution to boil without evaporation.

5.2.3. Heat the slides in a microwave for 20 min at approximately 675–700 watts. Check the slides regularly and replace evaporated liquid with diH2O such that sections remain submerged in unmasking solution at all times.

5.2.4. Allow slides to cool down in solution for 1 h at room temperature.

5.3. Dissolve 6 g of Fish Skin Gelatin (FSG) in 1 L of PBS. PBS/FSG is used as washing buffer. Prepare a blocking solution of 10% normal serum in PBS/FSG.

NOTE: Fish Skin Gelatin is used in the preparation of the blocking buffer. FSG does not contain serum proteins that can cross-react with mammalian antibodies, minimizing background noise. However, other blocking option should be preferred with biotin detection systems as FSG contains endogenous biotin. The type of normal serum used is based on the secondary antibody used. When donkey secondary antibodies are used, normal horse serum should be selected for blocking and antibody dilutions.

5.4. Incubate slides in PBS for 5 min at room temperature. Circle tissue sections with a hydrophobic pen. Cover the sections with the blocking buffer PBS/FSG/normal serum for 1 h at

room temperature. Prepare the primary antibody solution in PBS/FSG/normal serum during this step while the tissues are blocking.

5.5. Incubate with primary antibodies diluted in PBS/FSG/normal serum overnight at 4 °C in a humidity chamber. One section per slide should be incubated with a mix of IgG control antibodies at the same concentration as the primary antibodies to control for primary antibody specificity.

5.6. Wash the slides as follows at room temperature: PBS/FSG for 5 min (3x), then PBS for 5 min (1x).

5.7. Incubate with fluorophore-conjugated secondary antibodies (see **Table of Materials**) and diamidino-2-phenylindole (DAPI) for nucleus counterstaining diluted in PBS/FSG/normal serum for 1 h at room temperature. Protect slides from light.

5.8. Wash slides as described in step 5.6.

5.9. Mount slides using mounting media suitable for fluorescence (see **Table of Materials**).

6. **Confocal microscopy**

NOTE: The use of a confocal microscope and z-stack acquisition is critical for single-cell counting.

6.1.1. Set acquisition parameters to be used throughout the study: image resolution (1024x1024 or 2048x2048 pixels); Optical path and number of channels, which are a function of the combination of secondary antibodies selected; scanning speed (recommended scanning speed: 7-8); and differential interference contrast (DIC) channel.

6.2. Using sections stained with the primary antibodies and IgG control, set the detector sensitivity, laser power, and offset for each individual channel. The IgG control is used to minimize the background signal.

6.3. Set up the upper and lower positions for z-stack acquisition. Predetermine the thickness and number of stacks to acquire. These parameters should remain consistent throughout the study.

NOTE: We recommend imaging 8 to 10 stacks of 1 µm thickness. Stay consistent in the number of stacks imaged throughout the study.

6.4. Image tissue sections stained with primary antibodies and IgG control for all channels including DIC.

6.5. Label at least one image with a scale bar for image calibration during single cell counting.

7. Single cell counting

7.1. Install and open ImageJ. If necessary, download **Plugins** in the section **Download** > **Input/Output** of the ImageJ website to open the image file generated depending of the format of the images generated by the confocal microscope.

7.2. Open the image file in ImageJ.

7.3. Calibrate the image with a reference scale bar using the image generated in **6.6**.

7.4. Delineate the region of interest in which single cell counting will be performed using the DIC channel (**Figure 4**).

NOTE: One region can be delineated at a time. Depending of the experimental questions, single cell counting can be performed in the entire lesion area (see **7.3.1**) and/or in a sublocation of the lesion. For example, investigation of the fibrous cap area (see **7.3.2**) is particularly relevant since its cellular composition is an important index of lesion propensity to rupture.

7.4.1. Delineate the lesion area by following the lumen border (**Figure 4A**; white arrows) and the internal elastic lamina (**Figure 4A**; yellow arrows) visible on the DIC image.

7.4.2. For analysis of the fibrous cap area, determine the border distant of 30 µm from the lumen and trace the border (**Figure 4B-D**).

NOTE: The fibrous cap area is classically defined as the region enriched in ACTA2+ cells and collagen underlaying the lumen (**Figure 4B**). The enrichment in ACTA2+ cell and collagen plays a critical role in lesion stability. Previous studies have determined that the ACTA2+ cell rich fibrous cap area averages a thickness of 30 µm from the lumen in SMC-lineage tracing $ApoE^{-/-}$ mice fed a high-fat diet for 18 to 26 weeks (**Figure 4C**). Thus, meticulous characterization of the effects of genetic manipulation or pharmacological treatment on the fibrous cap area cellular composition is remarkably relevant.

7.5. Open the **Channels Tools** panel (**Image** > **Color** > **Channel Tools**) and pseudo-color the different staining channels (**Figure 5A**; box 1).

7.6. Merge the color channels (**Image** > **Color** > **Merge Colors**) (**Figure 5A**; box 2). All channels should be visible on the same image (**Figure 5B**). Turn on and off individual color channels using the **Channel Tool**s panel (**Figure 5A**; box 1).

7.7. Set up the counting tool.

7.7.1. Right click on the **Counting** icon in the tool bar (**Figure 5C**; box 1) and select **Multi-Point Tool**.

7.7.2. Double click on the same icon to open the **Point Tool** panel (**Figure 5C**; box 2).

7.7.3. Select the type and size of the items used to count cells.

7.7.4. Check **Show all**.

7.8. Turn on the DAPI channel only in the **Channel Tools** panel and select the Counter channel 0 (**Figure 5C**; box 3). Click on individual nuclei that will be tagged (e.g., yellow dots in **Figure 5C-D**). Scroll z-stacks to count all nuclei stained in the region of interest. The number of events is indicated below the counter channel in **Point Tool** panel (**Figure 5C**; box 4).

7.9. Turn on another staining channel (e.g., eYFP staining). Select the Counter channel 1. Click cells in which there is a colocalization between DAPI and staining. For cytoplasmic staining, select cells for with staining surrounds the nucleus on the entire depth of the nucleus (check several z-stacks).

7.10. Repeat by modifying the staining combinations and selecting new Counter channels to count the cell populations of interest. Every dot color represents a different cell population (**Figure 5D**). Results can be expressed as number of cells to total number of DAPI or number of cells to region area.

REPRESENTATIVE RESULTS:

Myh11-Cre/ERT2 R26R-EYFP Apoe$^{-/-}$ mice were injected with tamoxifen between six and eight weeks of age before being fed a high fat diet. At 18 weeks of high fat diet feeding, two groups of eight mice were treated weekly with either a mouse monoclonal anti-IL-1β antibody or an isotype-matched IgG control at 10 mg/kg for 8 weeks (**Figure 1**)[7]. Mice were sacrificed and perfused with a 4% PFA-PBS solution. Brachiocephalic arteries were dissected, processed, and sectioned as described above (**Figure 2** and **Figure 3**).

After immunofluorescent staining with antibodies targeting the lineage tracing reporter (YFP) and phenotypic markers (ACTA2, LGALS3, RUNX2), a thickness of 8-10 µm of the BCA cross sections was imaged using a confocal microscope. Images of each individual staining, DAPI (nuclear staining), and DIC were acquired. Delineation of regions of interest for single cell counting (lesion, fibrous cap) was performed using DIC images (**Figure 4**). Single cell counting to determine the abundance of different SMC-derived populations was performed using ImageJ (**Figure 5**).

We present two representative immunofluorescent staining and single counting assessing the effect of IL-1β inhibition on cellular composition in advanced atherosclerotic lesions. First, staining was done for the SMC lineage tracing reporter YFP, the SMC marker ACTA2, and the macrophage marker LGALS3 in cross sections at two different locations of the BCA (480 µm and 780 µm from the aortic arch) (**Figure 6**). Single cell counting analysis in the fibrous cap region of these cross section were performed, and remarkable differences were found in the cellular composition of the fibrous cap area between mice treated with the anti-IL-1β antibody and mice treated with the isotype-matched IgG control (**Figure 6A**). Inhibition of IL-1β was associated with

a decrease in YFP+ SMC and an increase in LGALS3+ cells (**Figure 6B**). Regarding the phenotypes of SMC populations, a decrease in the number of YFP+ACTA2+ SMC was observed, whereas the relative number of SMC-derived macrophages (YFP+LGALS3+) was significantly increased at both BCA locations (**Figure 6C**).

Finally, we investigated the effect of IL-1β inhibition on the SMC phenotypic transition into chondrogenic cells. This phenotypic transition is an important driver of vascular calcification, major feature of late-stage atherosclerosis[14,32,33]. BCA cross-sections were stained for the SMC lineage tracing reporter YFP, the osteochondrogenic marker RUNX2, and the macrophage marker LGALS3 (**Figure 7A**). The abundance and the origin of the RUNX2+ chondrogenic cells were characterized within the lesion area in our two experimental groups. We found that inhibition of IL-1β did not impact the overall number of RUNX2+ cells within the lesion, nor the proportion of SMC-derived (YFP+RUNX2+) and macrophage-derived (YFP-LGALS3+RUNX2+) chondrogenic cells (**Figure 7B**).

FIGURE AND TABLE LEGENDS:

Figure 1: Intervention studies in Smooth Muscle cell lineage tracing mice. (**A**) Schematic representation of the *Myh11*-Cre/ERT2 R26R-EYFP Apoe$^{-/-}$ tamoxifen-inducible SMC specific lineage tracing mouse model. Treatment with tamoxifen induces recombination of the R26R-YFP locus and the excision of a STOP codon and the permanent expression of YFP by SMC. (**B**) Schematic of intervention studies in which *Myh11*-Cre/ERT2 R26R-EYFP Apoe$^{-/-}$ mice fed a Western diet for 18 weeks were injected weekly with the IL-1β antibody or an isotype-matched IgG control antibody at a concentration of 10 mg/kg for 8 weeks.

Figure 2: Brachiocephalic artery dissection. (**A**) Schematic of a gravity driven perfusion system. The system is set up at a precise height allowing perfusion at a pressure close to the average systolic blood pressure in mice. The pressure slightly varies with volume height as liquid is used during perfusion between height h_1 and h_2. (**B**) Equation for calculation of the pressure of static fluids and determination of the height to reach a pressure of perfusion equal to the C57Bl6 mouse average systolic blood pressure. (**C**) Pictures of the proximal aorta and branching arteries in C57Bl6 mouse fed a chow diet (left picture) and Apoe$^{-/-}$ mouse fed a high fat diet for 26 weeks (right picture). The asterisk indicates the presence of atherosclerotic lesions. (**D**) Schematic of the proximal aorta and branching arteries. Red arrows represent cuts for isolation of the right carotid and brachiocephalic artery isolation and numbers indicate the order of the cuts.

Figure 3: Tissue processing, embedding, and sectioning. (**A**) Photograph of an embedding cassette with BCA tissue. The BCA is positioned on a foam pad. (**B**) Zoom-in of the BCA positioned on the foam pad. The BCA is oriented with the aortic arch close to the label part of the cassette and the carotid straightened vertically. Scale bar: 1 cm. (**C**) Schematic of paraffin block after embedding of the brachiocephalic artery. (**D**) Schematic of serial slides with 10 µm-thick serial sections with indication of the distance from the aortic arch.

Figure 4: Delineation of the atherosclerotic lesion and fibrous cap area. (**A)** Representative

micrographs of DIC image atherosclerotic lesion in brachiocephalic artery cross-sections from *Myh11*-Cre/ERT2 R26R-EYFP Apoe$^{-/-}$. The luminal and the internal elastic lamina borders are localized by white and yellow arrows, respectively (left panel). The lesion area is delineated by a dashed line (right panel) Scale bar: 100 µm. (**B**) Representative micrographs of DIC and ACTA2 staining. Double-head arrows show the thickness of the ACTA2 staining within the area underlaying the lumen defining the fibrous cap area. (**C**) Quantification of the subluminal ACTA2^{+} thickness in *Myh11*-Cre/ERT2 R26R-EYFP Apoe$^{-/-}$ fed a high-fat diet for 18, 21 and 26 weeks. Using this strain of mice, the fibrous cap has an average thickness of 25-30 µm in advance atherosclerotic lesions. Results are expressed as mean ± SEM. (**D**) Delineation of a fixed 30 µm thick fibrous cap area for single cell counting.

Figure 5: Single cell counting using ImageJ. Screen captures illustrating key steps of single cell counting with ImageJ on images acquired by confocal microscopy. (**A**) Each individual staining channel and individual z-stack are visible by scrolling c: and z: bars at the bottom of the image. Staining channels are pseudo-colored using the Channel panel (**1**) Staining channels (YFP, LGALS3, ACTA2, DAPI for nuclear staining and DIC) are merged using the Merge Channel panel (**2**). (**B**) Results of channel merging for YFP, LGALS3, ACTA2, DAPI, and DIC. (**C**) Nucleus counting based on DAPI staining using the Counting icon (**1**) and Point Tool panel (**2**). A different counter channel is used for each cell population (**3**). The number of events counted is indicated below the counter channel (**4**). White rectangle: region enlarged on the right. (**D**) Representative image of single cell counting within the fibrous cap area (dashed line) for multiple cell populations including DAPI (yellow dots), YFP^{+} cells (magenta dots), YFP^{-}LGALS3^{+} cells (cyan dots), YFP^{+}LGALS3^{+} cells (orange dots), YFP^{+}ACTA2^{+} cells (green dots), and YFP^{-}ACTA2^{+} cells (dark blue dots). White rectangle: region enlarged on the right.

Figure 6: Characterization of the effects of IL-1β inhibition on the cellular composition of the fibrous cap area at two distinct BCA locations of SMC lineage tracing Apoe-/- mice. (**A**) BCA cross sections at 480 µm and 780 µm from the aortic arch from mice treated with the IL-1β antibody or the IgG control as shown in **Figure 1** were stained for YFP, LGALS3, and DAPI (nuclear staining) and the section was imaged by DIC. Immunofluorescent channels were merged (bottom right panels). The dashed lines delineate the fibrous cap regions. Scale bars: 100 µm. (**B**) Single cell counting reveals that inhibition of IL-1β is associated with a significant decrease in YFP^{+} cells and an increase in LGALS3^{+} cells within the fibrous cap area. **C**) Within the YFP^{+} cell population, a decrease in YFP^{+}ACTA2^{+} and an increase in YFP^{+}LGALS3^{+} populations are observed. Results are expressed as mean ± SEM. Statistical analysis: unpaired multiple t-test.

Figure 7: Effect of IL-1β inhibition on the number of RUNX2+ chondrogenic cells with advanced atherosclerotic lesions. A) BCA cross sections are stained for YFP, LGALS3, RUNX2 and DAPI (nuclear staining), and all channels were merged (bottom panels). The dashed lines delineate the lesion area. Scale bars: 100 µm. **B**) Single cell counting shows that inhibition of IL-1β does not impact the total number of RUNX2^{+} cells within the lesion nor the proportion of RUNX2^{+} cells from SMC origin (YFP^{+}RUNX2^{+}; YFP^{+}LGALS3^{+}RUNX2^{+}) and myeloid origin (YFP^{-}LGALS3^{+}RUNX2^{+}). Results are expressed as mean ± SEM. Statistical analysis: Unpaired multiple t-test.

DISCUSSION:

Despite decades of research and technical advances in studying atherosclerosis, the field has a disappointing history of translating scientific findings to clinical therapies[34,35]. This phenomenon may be explained in part by discrepancies in animal models, experimental designs, and lesion analyses. Herein, we describe an experimental pipeline that we used to analyze the cellular composition in advanced atherosclerotic lesions using lineage tracing mice[7]. This method allows for a meticulous investigation of cell fate mapping and phenotyping, which are key parameters controlled by potential mechanisms at play in advanced atherosclerotic lesions.

The SMC-lineage tracing mouse model is a powerful tool to accurately track the fate and phenotypic modulations of this lineage and their contribution to atherosclerosis pathogenesis. The tamoxifen-inducible *Cre-loxP* system enables labeling of mature vascular SMC expressing MYH11 prior to the initiation of atherosclerosis. Compelling evidence using this system has demonstrated that atherosclerotic plaques are highly plastic and vascular SMC can undergo phenotypic switching, losing their contractile phenotype and SMC-specific markers, proliferating, migrating, and even transdifferentiating into macrophage-like cells[17,18]. In the present protocol, we show how lineage-tracing detection and immunofluorescent staining for markers of interest can be integrated to precisely determine phenotypic transitions undertaken by SMC and their relative frequency among other SMC populations.

This methodology is highly complementary with other assays frequently performed in the field. First, assessment of atherosclerotic lesion burden by *en face* aortic preparations combined with lipid staining by Sudan IV is widely used due to its convenience and speed. However, this is an inadequate measure of key morphological parameters such as lesion size, lumen size, and vessel remodeling. Staining of *en face* aortic preparation by Sudan IV to visualize lipid deposition can be used to quantify relative lesion area within the aorta, but it can provide inconsistent staining of lesions, as only the neutral lipid component is visualized while regions occupied by other constituents, such as extracellular matrix, usually are neglected[8]. Moreover, *en face* staining is unable to inform about the lesion morphology and cannot distinguish between fatty streaks and advanced lesions. Vessel morphology is an important parameter used for evaluating atherosclerosis stage and rupture risk, including lesion size, lumen diameter, vessel remodeling[7,36,37]. These analyses require the conservation of the vessel morphology for proper quantification. Importantly, protocols for investigation of morphological parameters greatly overlap with the protocol detailed here. In particular, they rely on the use of a gravity-driven vascular perfusion system for PBS and fixative perfusion to provide greater consistency in the pressure applied. The gravity-driven infiltration system guarantees a constant flow speed and pressure between each independent mouse and prevents the inconsistency of manual force-driven perfusion between independent experiments or researchers. The gravity perfusion system should be set up to induce perfusion at a pressure near the average murine blood pressure (70-120 mmHg). Second, we provided a standardized and systematic method of embedding and sectioning for the brachiocephalic artery. By defining the start site of sectioning and quantifying the lesion area at multiple locations throughout the brachiocephalic artery, we can limit the

random variation that comes with limited sampling.

Flow cytometry is another technique highly complementary with immunofluorescent staining coupled with single cell counting that has been widely used in quantifying cell populations within atherosclerotic lesions[38]. It consists of the digestion of mouse aorta and labeling of the released cells with fluorescent antibodies. Flow cytometry offers a quantitative analysis of the cellular populations present in the aorta. However, like all technologies, flow cytometry has limitations. Despite the distinct benefit of fitting a large array of simultaneous markers, there is a complete loss of spatial resolution, and it becomes unclear whether a cell population is enriched in the fibrous cap or the necrotic core. Additionally, there is a risk of dilution effect since flow cytometry requires a large number of cells and often does not focus only on atherosclerotic areas. For this reason, immunofluorescence and flow cytometry can be used in a complementary manner to allow for both high dimensional profiling and lesion localization.

Finally, the protocol is focused on the quantification of SMC populations in BCA advanced lesion using paraformaldehyde-fixed and paraffin-embedded tissue sections. However, this protocol can be used to investigate other vascular beds including the aortic root or the abdominal aorta, two vascular territories subject to atherosclerosis development. Systematic processing and sectioning of the aortic root have been previously well described[8,39]. As atherosclerosis develops at different locations and that genetic manipulation or therapeutic intervention can non-homogenously impact these sites[21], it is important to investigate as many vascular beds as possible to draw accurate conclusions. Immunofluorescent staining and single cell counting can also be performed using frozen sections. This might be necessary due to the incompatibility of antibodies with paraffin sections. Although the animal perfusion and tissue embedding will differ from this protocol, investigators can follow the rest of the experimental procedures described here.

In conclusion, the techniques described here outline a systematic approach to analyzing lesion cell populations and phenotypes in late-stage murine atherosclerosis. This protocol can serve as a template to investigate lesion populations by immunofluorescent staining in all types of experimental design including early and late-stage atherosclerosis, as well as prevention and intervention studies.

ACKNOWLEDGMENTS:

We thank the Center for Biologic Imaging (CBI) at the University of Pittsburgh for their assistance. This work was supported by is supported by Scientific Development Grant 15SDG25860021 from the American Heart Association to D.G. R.A.B. was supported by NIH grant F30 HL136188.

DISCLOSURES:

The authors have nothing to disclose.

REFERENCES:

1 GBD DALYs and HALE Collaborators. Global, regional, and national disability-adjusted life-years (DALYs) for 315 diseases and injuries and healthy life expectancy (HALE), 1990-2015: a systematic analysis for the Global Burden of Disease Study 2015. *Lancet.* **388** (10053), 1603-1658, doi:10.1016/S0140-6736(16)31460-X (2016).

2 Benjamin, E. J. et al. Heart Disease and Stroke Statistics-2018 Update: A Report From the American Heart Association. *Circulation.* **137** (12), e67-e492, doi:10.1161/CIR.0000000000000558 (2018).

3 Hay, M., Thomas, D. W., Craighead, J. L., Economides, C., Rosenthal, J. Clinical development success rates for investigational drugs. *Nature Biotechnology.* **32** (1), 40-51, doi:10.1038/nbt.2786 (2014).

4 Bhaskar, V. et al. Monoclonal antibodies targeting IL-1 beta reduce biomarkers of atherosclerosis in vitro and inhibit atherosclerotic plaque formation in Apolipoprotein E-deficient mice. *Atherosclerosis.* **216** (2), 313-320, doi:10.1016/j.atherosclerosis.2011.02.026 (2011).

5 Isoda, K. et al. Lack of interleukin-1 receptor antagonist modulates plaque composition in apolipoprotein E-deficient mice. *Arteriosclerosis, Thrombosis, and Vascular Biology.* **24** (6), 1068-1073, doi:10.1161/01.ATV.0000127025.48140.a3 (2004).

6 Kirii, H. et al. Lack of interleukin-1beta decreases the severity of atherosclerosis in ApoE-deficient mice. *Arteriosclerosis, Thrombosis, and Vascular Biology.* **23** (4), 656-660, doi:10.1161/01.ATV.0000064374.15232.C3 (2003).

7 Gomez, D. et al. Interleukin-1β has atheroprotective effects in advanced atherosclerotic lesions of mice. *Nature Medicine.* **24**, 1418-1429, doi:10.1038/s41591-018-0124-5 (2018).

8 Daugherty, A. et al. Recommendation on Design, Execution, and Reporting of Animal Atherosclerosis Studies: A Scientific Statement From the American Heart Association. *Circulation Research.* **121** (6), e53-e79, doi:10.1161/RES.0000000000000169 (2017).

9 Baylis, R. A., Gomez, D., Owens, G. K. Shifting the Focus of Preclinical, Murine Atherosclerosis Studies From Prevention to Late-Stage Intervention. *Circulation Research.* **120** (5), 775-777, doi:10.1161/CIRCRESAHA.116.310101 (2017).

10 Kolodgie, F. D. et al. Pathologic assessment of the vulnerable human coronary plaque. *Heart.* **90** (12), 1385-1391, doi:10.1136/hrt.2004.041798 (2004).

11 Virmani, R., Kolodgie, F. D., Burke, A. P., Farb, A., Schwartz, S. M. Lessons from sudden coronary death: a comprehensive morphological classification scheme for atherosclerotic lesions. *Arteriosclerosis, Thrombosis, and Vascular Biology.* **20** (5), 1262-1275 (2000).

12 Gomez, D., Owens, G. K. Smooth muscle cell phenotypic switching in atherosclerosis. *Cardiovascular Research.* **95** (2), 156-164, doi:10.1093/cvr/cvs115 (2012).

13 Owens, G. K., Kumar, M. S., Wamhoff, B. R. Molecular regulation of vascular smooth muscle cell differentiation in development and disease. *Physiological Reviews.* **84** (3), 767-801, doi:10.1152/physrev.00041.2003 (2004).

14 Speer, M. Y. et al. Smooth muscle cells give rise to osteochondrogenic precursors and chondrocytes in calcifying arteries. *Circulation Research.* **104** (6), 733-741, doi:10.1161/CIRCRESAHA.108.183053 (2009).

15 Gomez, D., Shankman, L. S., Nguyen, A. T., Owens, G. K. Detection of histone modifications at specific gene loci in single cells in histological sections. *Nature Methods.* **10** (2), 171-177, doi:10.1038/nmeth.2332 (2013).
16 Feil, S. et al. Transdifferentiation of vascular smooth muscle cells to macrophage-like cells during atherogenesis. *Circulation Research.* **115** (7), 662-667, doi:10.1161/CIRCRESAHA.115.304634 (2014).
17 Shankman, L. S. et al. KLF4-dependent phenotypic modulation of smooth muscle cells has a key role in atherosclerotic plaque pathogenesis. *Nature Medicine.* **21**, 628, doi:10.1038/nm.3866 (2015).
18 Cherepanova, O. A. et al. Activation of the pluripotency factor OCT4 in smooth muscle cells is atheroprotective. *Nature Medicine.* **22**, 657, doi:10.1038/nm.4109 (2016).
19 Albarran-Juarez, J., Kaur, H., Grimm, M., Offermanns, S., Wettschureck, N. Lineage tracing of cells involved in atherosclerosis. *Atherosclerosis.* **251**, 445-453, doi:10.1016/j.atherosclerosis.2016.06.012 (2016).
20 Chappell, J. et al. Extensive Proliferation of a Subset of Differentiated, yet Plastic, Medial Vascular Smooth Muscle Cells Contributes to Neointimal Formation in Mouse Injury and Atherosclerosis Models. *Circulation Research.* **119** (12), 1313-1323, doi:10.1161/CIRCRESAHA.116.309799 (2016).
21 Newman, A. A. et al. Irradiation abolishes smooth muscle investment into vascular lesions in specific vascular beds. *JCI Insight.* **3** (15), doi:10.1172/jci.insight.121017 (2018).
22 Dobnikar, L. et al. Disease-relevant transcriptional signatures identified in individual smooth muscle cells from healthy mouse vessels. *Nature Communications.* **9** (1), 4567, doi:10.1038/s41467-018-06891-x (2018).
23 Misra, A. et al. Integrin beta3 regulates clonality and fate of smooth muscle-derived atherosclerotic plaque cells. *Nature Communications.* **9** (1), 2073, doi:10.1038/s41467-018-04447-7 (2018).
24 Majesky, M. W. et al. Differentiated Smooth Muscle Cells Generate a Subpopulation of Resident Vascular Progenitor Cells in the Adventitia Regulated by Klf4. *Circulation Research.* **120** (2), 296-311, doi:10.1161/CIRCRESAHA.116.309322 (2017).
25 Herring, B. P., Hoggatt, A. M., Burlak, C., Offermanns, S. Previously differentiated medial vascular smooth muscle cells contribute to neointima formation following vascular injury. *Vascular Cell.* **6**, 21, doi:10.1186/2045-824X-6-21 (2014).
26 Sheikh, A. Q., Misra, A., Rosas, I. O., Adams, R. H., Greif, D. M. Smooth muscle cell progenitors are primed to muscularize in pulmonary hypertension. *Science Translational Medicine.* **7** (308), 308ra159, doi:10.1126/scitranslmed.aaa9712 (2015).
27 Bentzon, J. F., Majesky, M. W. Lineage tracking of origin and fate of smooth muscle cells in atherosclerosis. *Cardiovascular Research.* **114** (4), 492-500, doi:10.1093/cvr/cvx251 (2018).
28 Wirth, A. et al. G12-G13-LARG-mediated signaling in vascular smooth muscle is required for salt-induced hypertension. *Nature Medicine.* **14** (1), 64-68, doi:10.1038/nm1666 (2008).
29 Mattson, D. L. Comparison of arterial blood pressure in different strains of mice. *American Journal of Hypertension.* **14** (5 Pt 1), 405-408 (2001).

30 Whitesall, S. E., Hoff, J. B., Vollmer, A. P., D'Alecy, L. G. Comparison of simultaneous measurement of mouse systolic arterial blood pressure by radiotelemetry and tail-cuff methods. *American Journal of Physiology-Heart and Circulatory Physiology.* **286** (6), H2408-2415, doi:10.1152/ajpheart.01089.2003 (2004).
31 Durgin, B. G. et al. Smooth muscle cell-specific deletion of Col15a1 unexpectedly leads to impaired development of advanced atherosclerotic lesions. *American Journal of Physiology-Heart and Circulatory Physiology.* **312** (5), H943-H958, doi:10.1152/ajpheart.00029.2017 (2017).
32 Durham, A. L., Speer, M. Y., Scatena, M., Giachelli, C. M., Shanahan, C. M. Role of smooth muscle cells in vascular calcification: implications in atherosclerosis and arterial stiffness. *Cardiovascular Research.* **114** (4), 590-600, doi:10.1093/cvr/cvy010 (2018).
33 Lin, M. E. et al. Runx2 Deletion in Smooth muscle Cells Inhibits Vascular Osteochondrogenesis and Calcification but not Atherosclerotic Lesion Formation. *Cardiovascular Research.* doi:10.1093/cvr/cvw205 (2016).
34 Kilkenny, C., Browne, W. J., Cuthill, I. C., Emerson, M., Altman, D. G. Improving Bioscience Research Reporting: The ARRIVE Guidelines for Reporting Animal Research. *PLoS Biology.* **8** (6), doi:ARTN e1000412 10.1371/journal.pbio.1000412 (2010).
35 Landis, S. C. et al. A call for transparent reporting to optimize the predictive value of preclinical research. *Nature.* **490** (7419), 187-191, doi:10.1038/nature11556 (2012).
36 Nishioka, T. et al. Contribution of inadequate compensatory enlargement to development of human coronary artery stenosis: An in vivo intravascular ultrasound study. *Journal of the American College of Cardiology.* **27** (7), 1571-1576, doi:Doi 10.1016/0735-1097(96)00071-X (1996).
37 Pasterkamp, G. et al. Paradoxical Arterial-Wall Shrinkage May Contribute to Luminal Narrowing of Human Atherosclerotic Femoral Arteries. *Circulation.* **91** (5), 1444-1449 (1995).
38 Galkina, E. et al. Lymphocyte recruitment into the aortic wall before and during development of atherosclerosis is partially L-selectin dependent. *The Journal of Experimental Medicine.* **203** (5), 1273-1282, doi:10.1084/jem.20052205 (2006).
39 Venegas-Pino, D. E., Banko, N., Khan, M. I., Shi, Y., Werstuck, G. H. Quantitative analysis and characterization of atherosclerotic lesions in the murine aortic sinus. *Journal of Visual Experiments.* **82**, 50933, doi:10.3791/50933 (2013).

Figure 1

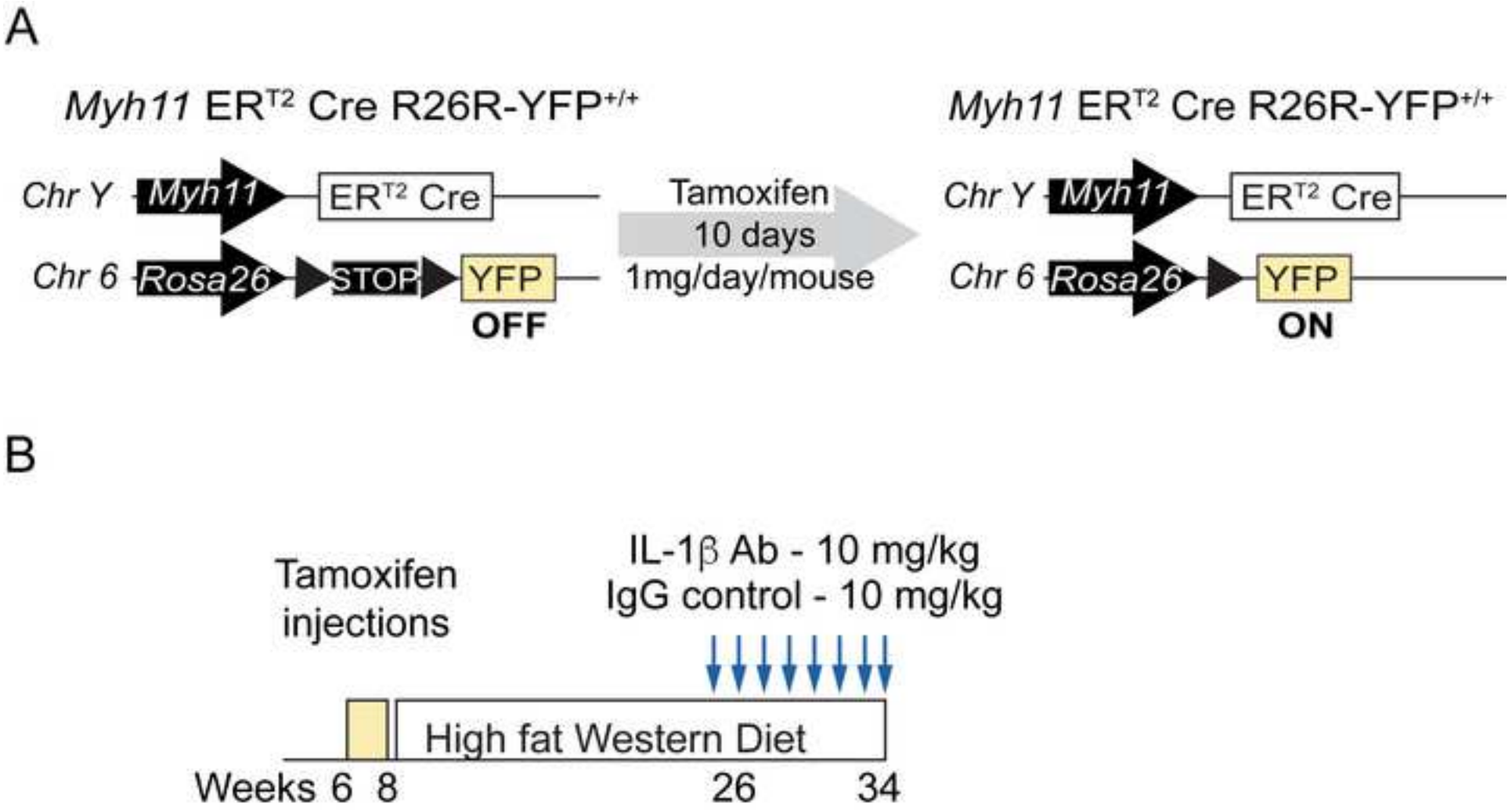

Figure 2

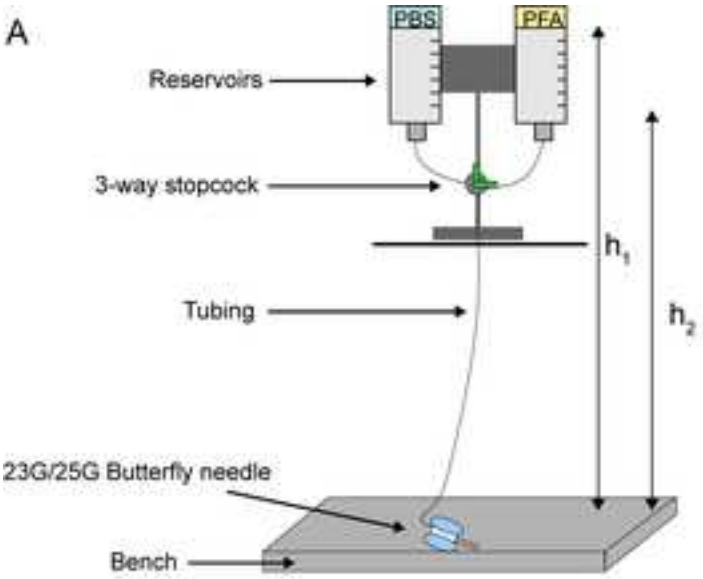

B

$P\ (kg/ms^2) = \rho\ (kg/m^3) \times g\ (m/s^2) \times h\ (m)$

P: Pressure
ρ: density of fluid
g: acceleration of gravity
h: height

Height to reach average systolic blood pressure (120 mmHg)

$$h_{max} = \frac{P_{sys}}{\rho \times g} = 1.6\ m$$

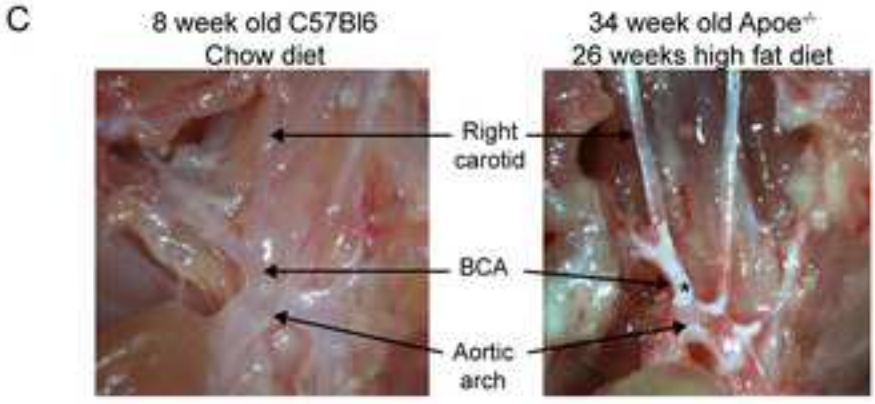

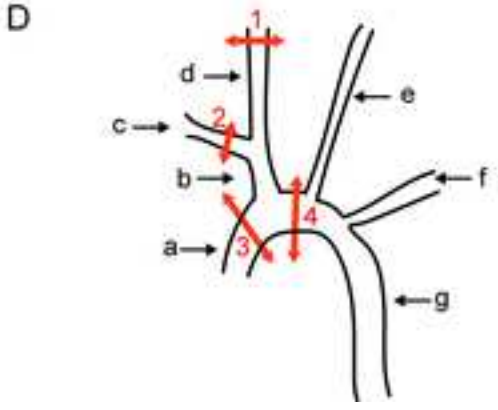

a: ascending aorta
b: brachiocephalic artery (BCA)
c: right subclavian artery
d: right carotid
e: left carotid
f: left subclavian artery
g: descending aorta

Figure 3

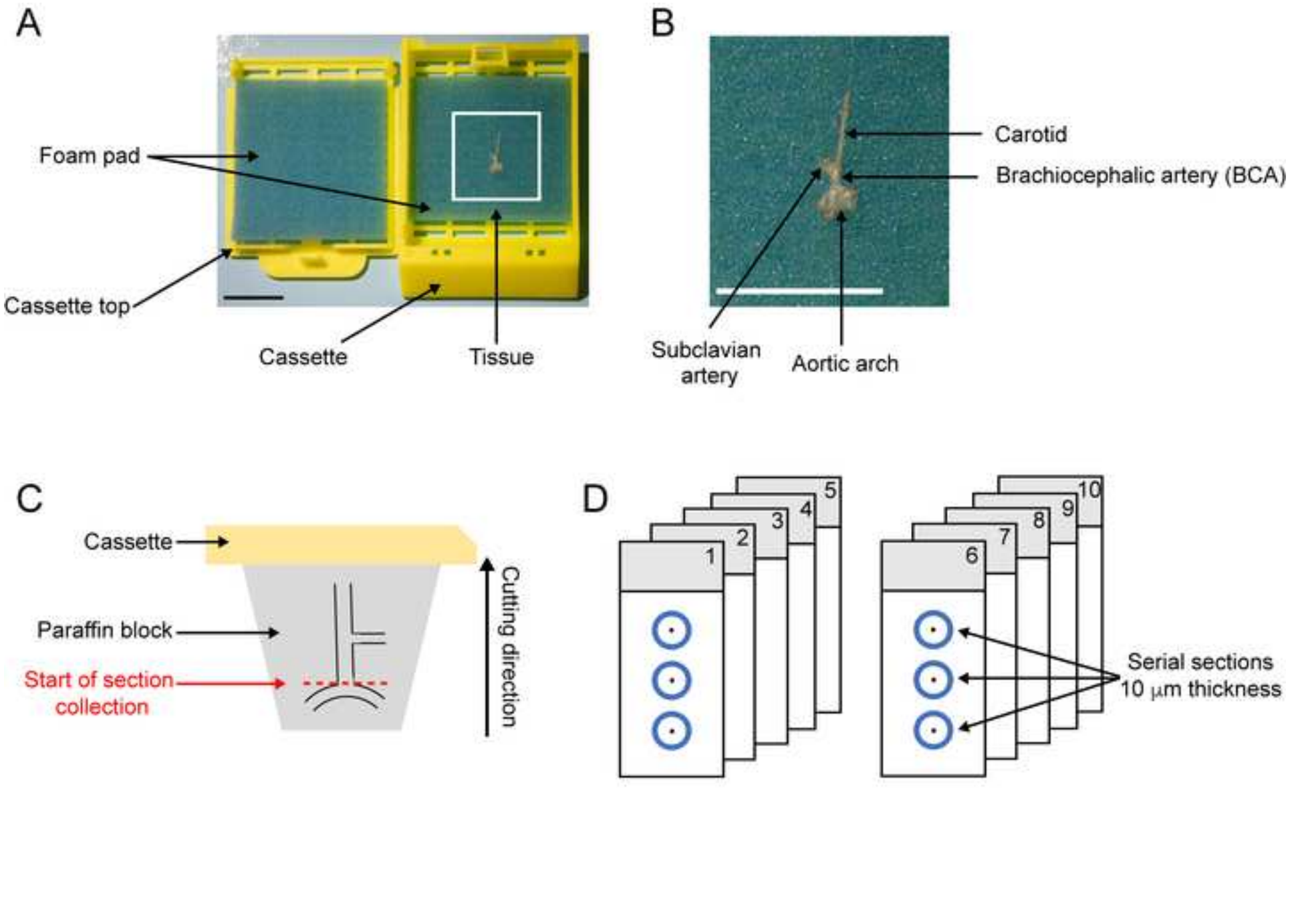

Figure 4

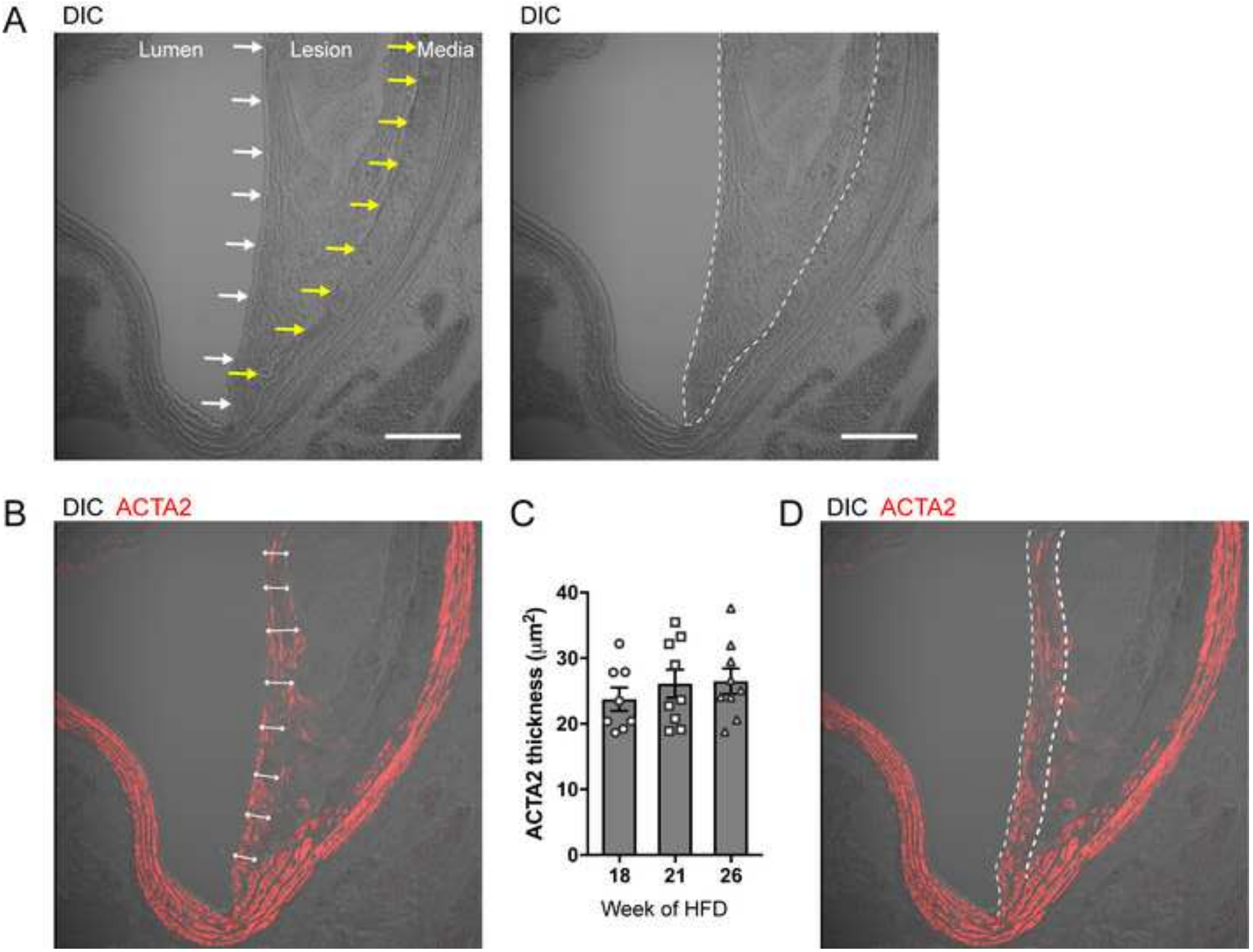

Figure 5

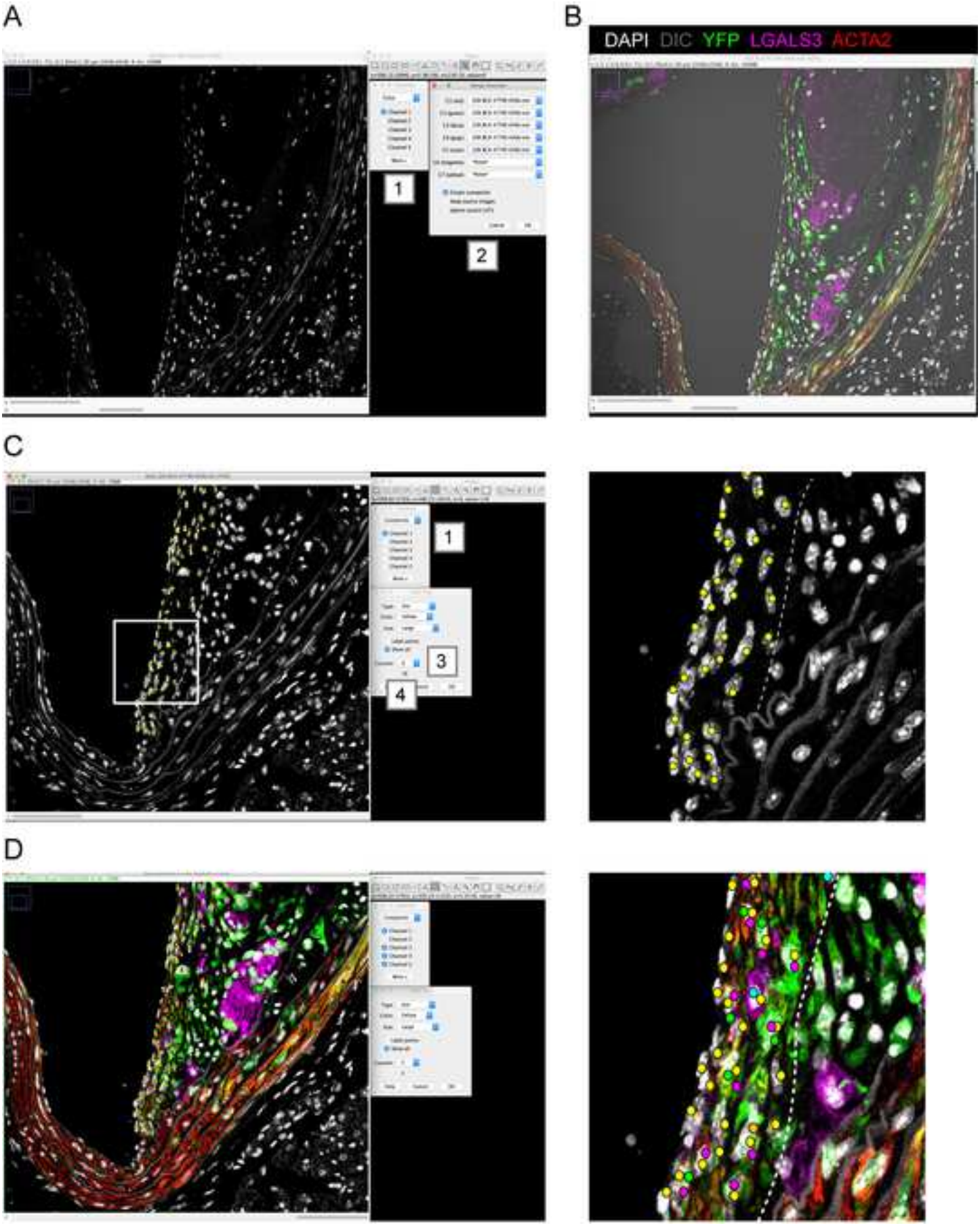

Figure 6

Click here to access/download;Figure;Figure 6.3.tif

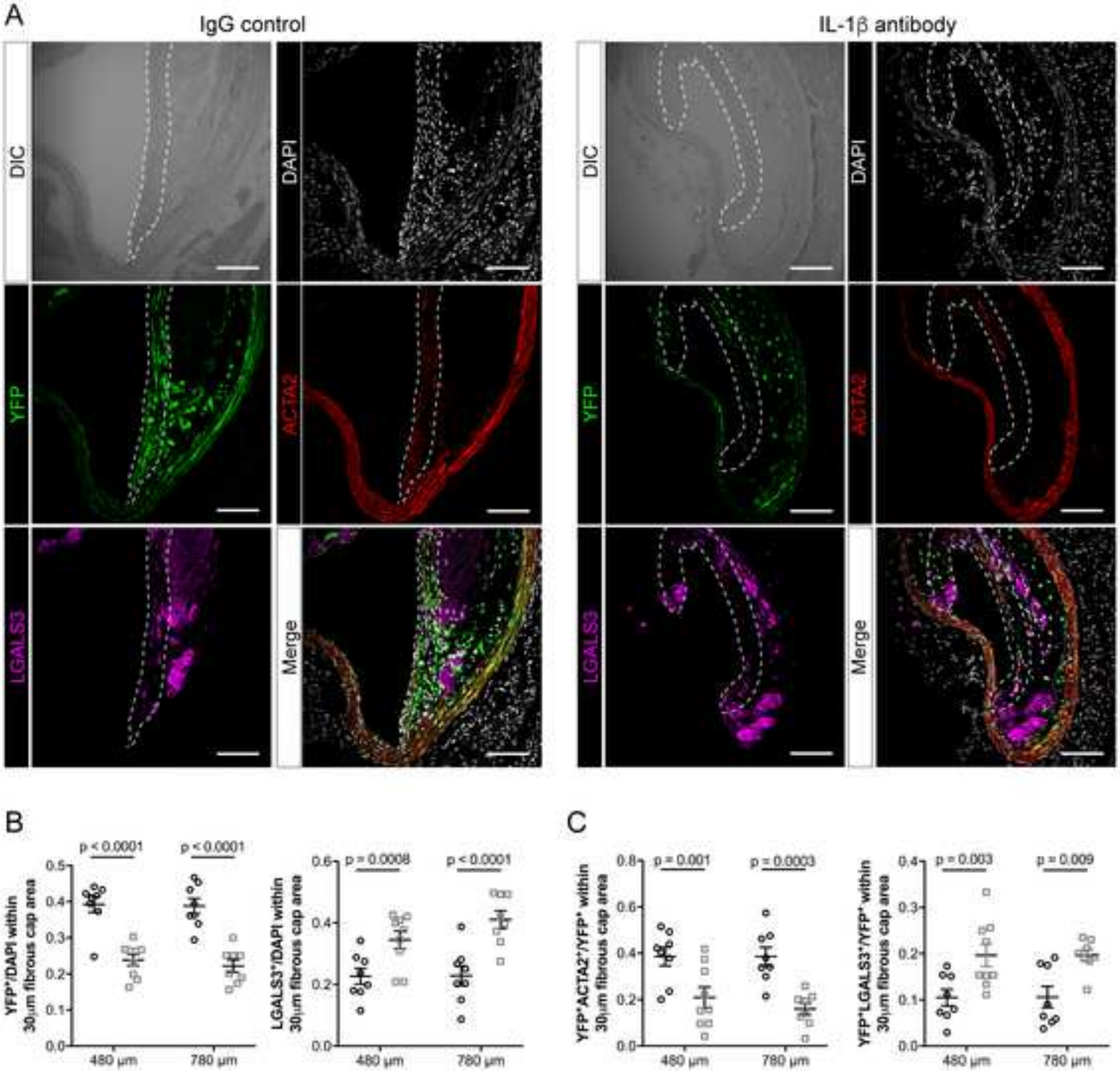

Figure 7

Click here to access/download;Figure;Figure 7.3.tif

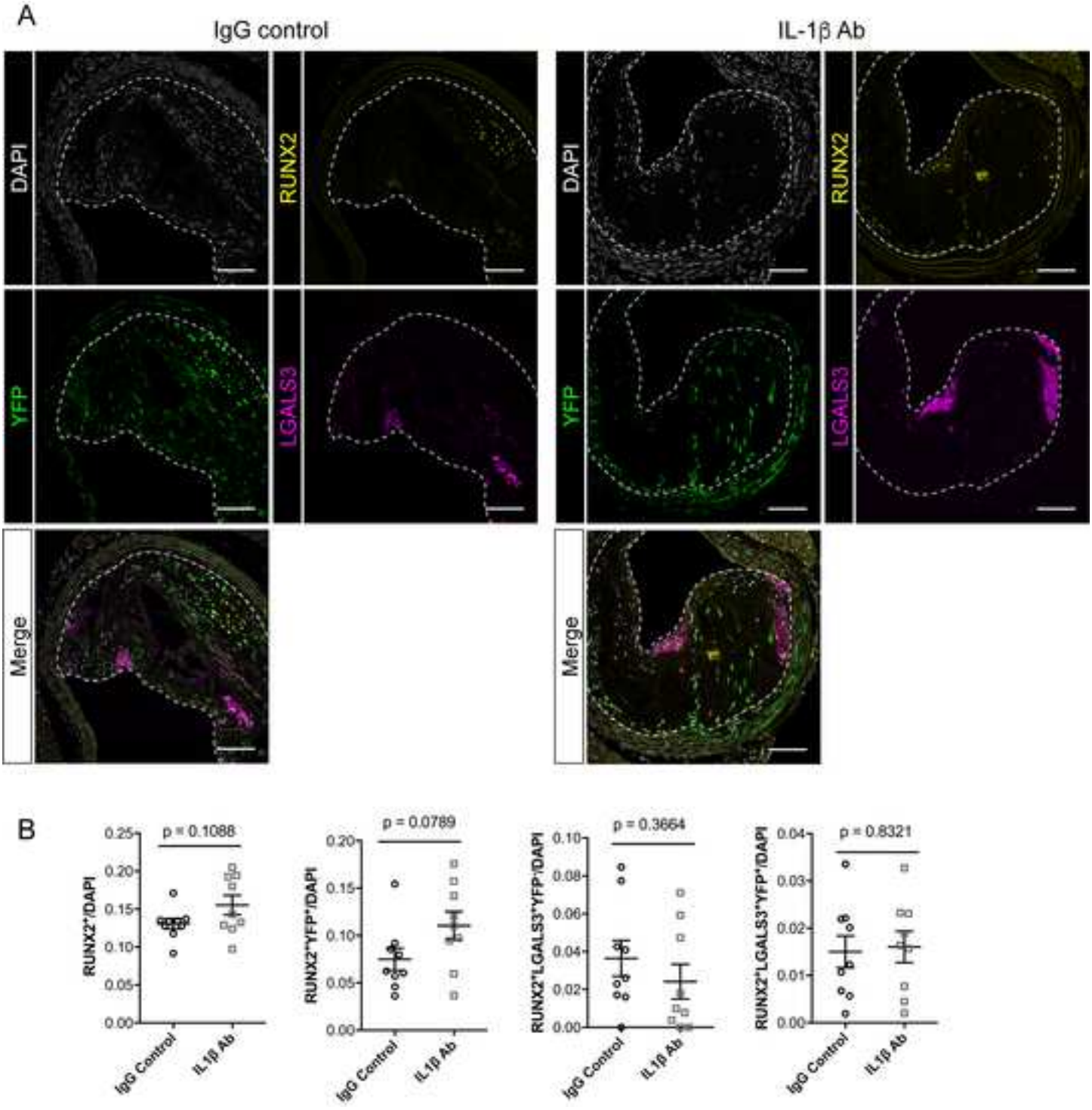

Name of Material/ Equipment	Company	Catalog Number	Comments/Description
16% Paraformaldehyde aqueous solution	Electron Microscopy Sciences	RT 15710	Tissue perfusion and fixation
23G butterfly needle	Fisher	BD367342	
25G needle	Fisher	14-821-13D	
A1 Confocal microscope	Nikon		Confocal microscope
ACTA2-FITC antibody (mouse)	Sigma Aldrich	F3777	Primary Antibody
Alexa-647 anti goat	Invitrogen	A-21447	Secondary antibody
Antigen Unmasking solution, Citric acid based	Vector Labs	H-3300	Antigen retrieval solution
Chow Diet	Harlan Teklad	TD.7012	
Coverslip	Fisher	12-544-14	Any 50 x 24 mm cover glass
DAPI (4',6-Diamidino-2-Phenylindole, Dihydrochloride)	Invitrogen	D1306	Nucleus fluorescent counterstaining
Donkey Alexa-488 anti-rabbit	Invitrogen	A-21206	Secondary antibody
Donkey Alexa-555 anti-rat	Abcam	ab150154	Secondary antibody
DPBS 10X without Calcium and Magnesium	Gibco	14200166	PBS for solution dilutions and washes. Dilute to 1x in deionized water
Embedding cassette	Fisher	15-182-701D	
ETDA vacuum tube	Fisher	02-685-2B	
Ethanol 200 proof	Decon	2701	
Foam pad	Fisher	22-222-012	
Gelatin from cold water fish skin	Sigma Aldrich	G7765	
GFP antibody (goat)	abcam	ab6673	Primary antibody

goat IgG control	Vector Labs	I-5000		IgG control
High Fat Diet	Harlan Teklad	TD.88137		
ImageJ	NIH			Computer program https://imagej.nih.gov/ij/
LGALS3 antibody (rat)	Cedarlane	CL8942AP		Primary antibody
LSM700 confocal microscope	Zeiss			Confocal microscope
Microscope Slides, Superfrost Plus	Fisher	12-550-15		
Microtome blades	Fisher	30-538-35		
Mouse IgG control	Vector Labs	I-2000		IgG control
NIS element imaging software	Nikon			Imaging software for z-stack image acquisition
Normal Horse serum	Sigma Aldrich	H1270		
Pap Pen	Fisher	50-550-221		
Peanut oil	Sigma	P2144		
Prolong gold Antifade mountant	Invitrogen	P36930		Mounting medium
Rabbit IgG control	Vector Labs	I-1000		IgG control
Rat IgG control	Vector Labs	I-4000		IgG control
RUNX2 antibody (rabbit)	Abcam	ab192256		Primary Antibody
Syringe	BD		309628	1 ml syringe
Tamoxifen	Sigma	T5648		
Xylene	Fisher	X55K-4		
Zen imaging software	Zeiss			Imaging software for z-stack image acquisition

jove JOURNAL OF VISUALIZED EXPERIMENTS

1 Alewife Center #200
Cambridge, MA 02140
tel. 617.945.9051
www.jove.com

ARTICLE AND VIDEO LICENSE AGREEMENT

Title of Article: Quantitative analysis of cellular composition in atherosclerotic lesions of smooth muscle cell lineage-tracing mice

Author(s): Sidney Mahan, Mingjun Liu, Richard A. Baylis, Delphine Gomez

Item 1 (check one box): The Author elects to have the Materials be made available (as described at http://www.jove.com/**author**) via: [X] Standard Access [ ] Open Access

Item 2 (check one box):

[X] The Author is NOT a United States government employee.

[ ] The Author is a United States government employee and the Materials were prepared in the course of his or her duties as a United States government employee.

[ ] The Author is a United States government employee but the Materials were NOT prepared in the course of his or her duties as a United States government employee.

ARTICLE AND VIDEO LICENSE AGREEMENT

1. Defined Terms. As used in this Article and Video License Agreement, the following terms shall have the following meanings: "**Agreement**" means this Article and Video License Agreement; "**Article**" means the article specified on the last page of this Agreement, including any associated materials such as texts, figures, tables, artwork, abstracts, or summaries contained therein; "**Author**" means the author who is a signatory to this Agreement; "**Collective Work**" means a work, such as a periodical issue, anthology or encyclopedia, in which the Materials in their entirety in unmodified form, along with a number of other contributions, constituting separate and independent works in themselves, are assembled into a collective whole; "**CRC License**" means the Creative Commons Attribution-Non Commercial-No Derivs 3.0 Unported Agreement, the terms and conditions of which can be found at: http://creativecommons.org/licenses/by-nc-nd/3.0/legalcode; "**Derivative Work**" means a work based upon the Materials or upon the Materials and other pre-existing works, such as a translation, musical arrangement, dramatization, fictionalization, motion picture version, sound recording, art reproduction, abridgment, condensation, or any other form in which the Materials may be recast, transformed, or adapted; "**Institution**" means the institution, listed on the last page of this Agreement, by which the Author was employed at the time of the creation of the Materials; "**JoVE**" means MyJove Corporation, a Massachusetts corporation and the publisher of *The Journal of Visualized Experiments;* "**Materials**" means the Article and / or the Video; "**Parties**" means the Author and JoVE; "**Video**" means any video(s) made by the Author, alone or in conjunction with any other parties, or by JoVE or its affiliates or agents, individually or in collaboration with the Author or any other parties, incorporating all or any portion of the Article, and in which the Author may or may not appear.

2. Background. The Author, who is the author of the Article, in order to ensure the dissemination and protection of the Article, desires to have the JoVE publish the Article and create and transmit videos based on the Article. In furtherance of such goals, the Parties desire to memorialize in this Agreement the respective rights of each Party in and to the Article and the Video.

3. Grant of Rights in Article. In consideration of JoVE agreeing to publish the Article, the Author hereby grants to JoVE, subject to **Sections 4** and **7** below, the exclusive, royalty-free, perpetual (for the full term of copyright in the Article, including any extensions thereto) license (a) to publish, reproduce, distribute, display and store the Article in all forms, formats and media whether now known or hereafter developed (including without limitation in print, digital and electronic form) throughout the world, (b) to translate the Article into other languages, create adaptations, summaries or extracts of the Article or other Derivative Works (including, without limitation, the Video) or Collective Works based on all or any portion of the Article and exercise all of the rights set forth in (a) above in such translations, adaptations, summaries, extracts, Derivative Works or Collective Works and (c) to license others to do any or all of the above. The foregoing rights may be exercised in all media and formats, whether now known or hereafter devised, and include the right to make such modifications as are technically necessary to exercise the rights in other media and formats. If the "Open Access" box has been checked in **Item 1** above, JoVE and the Author hereby grant to the public all such rights in the Article as provided in, but subject to all limitations and requirements set forth in, the CRC License.

4. Retention of Rights in Article. Notwithstanding the exclusive license granted to JoVE in **Section 3** above, the Author shall, with respect to the Article, retain the non-exclusive right to use all or part of the Article for the non-commercial purpose of giving lectures, presentations or teaching classes, and to post a copy of the Article on the Institution's website or the Author's personal website, in each case provided that a link to the Article on the JoVE website is provided and notice of JoVE's copyright in the Article is included. All non-copyright intellectual property rights in and to the Article, such as patent rights, shall remain with the Author.

5. Grant of Rights in Video – Standard Access. This **Section 5** applies if the "Standard Access" box has been checked in **Item 1** above or if no box has been checked in **Item 1** above. In consideration of JoVE agreeing to produce, display or otherwise assist with the Video, the Author hereby acknowledges and agrees that, Subject to **Section 7** below, JoVE is and shall be the sole and exclusive owner of all rights of any nature, including, without limitation, all copyrights, in and to the Video. To the extent that, by law, the Author is deemed, now or at any time in the future, to have any rights of any nature in or to the Video, the Author hereby disclaims all such rights and transfers all such rights to JoVE.

6. Grant of Rights in Video – Open Access. This **Section 6** applies only if the "Open Access" box has been checked in **Item 1** above. In consideration of JoVE agreeing to produce, display or otherwise assist with the Video, the Author hereby grants to JoVE, subject to **Section 7** below, the exclusive, royalty-free, perpetual (for the full term of copyright in the Article, including any extensions thereto) license (a) to publish, reproduce, distribute, display and store the Video in all forms, formats and media whether now known or hereafter developed (including without limitation in print, digital and electronic form) throughout the world, (b) to translate the Video into other languages, create adaptations, summaries or extracts of the Video or other Derivative Works or Collective Works based on all or any portion of the Video and exercise all of the rights set forth in (a) above in such translations, adaptations, summaries, extracts, Derivative Works or Collective Works and (c) to license others to do any or all of the above. The foregoing rights may be exercised in all media and formats, whether now known or hereafter devised, and include the right to make such modifications as are technically necessary to exercise the rights in other media and formats. For any Video to which this Section 6 is applicable, JoVE and the Author hereby grant to the public all such rights in the Video as provided in, but subject to all limitations and requirements set forth in, the CRC License.

7. Government Employees. If the Author is a United States government employee and the Article was prepared in the course of his or her duties as a United States government employee, as indicated in **Item 2** above, and any of the licenses or grants granted by the Author hereunder exceed the scope of the 17 U.S.C. 403, then the rights granted hereunder shall be limited to the maximum rights permitted under such statute. In such case, all provisions contained herein that are not in conflict with such statute shall remain in full force and effect, and all provisions contained herein that do so conflict shall be deemed to be amended so as to provide to JoVE the maximum rights permissible within such statute.

8. Likeness, Privacy, Personality. The Author hereby grants JoVE the right to use the Author's name, voice, likeness, picture, photograph, image, biography and performance in any way, commercial or otherwise, in connection with the Materials and the sale, promotion and distribution thereof. The Author hereby waives any and all rights he or she may have, relating to his or her appearance in the Video or otherwise relating to the Materials, under all applicable privacy, likeness, personality or similar laws.

9. Author Warranties. The Author represents and warrants that the Article is original, that it has not been published, that the copyright interest is owned by the Author (or, if more than one author is listed at the beginning of this Agreement, by such authors collectively) and has not been assigned, licensed, or otherwise transferred to any other party. The Author represents and warrants that the author(s) listed at the top of this Agreement are the only authors of the Materials. If more than one author is listed at the top of this Agreement and if any such author has not entered into a separate Article and Video License Agreement with JoVE relating to the Materials, the Author represents and warrants that the Author has been authorized by each of the other such authors to execute this Agreement on his or her behalf and to bind him or her with respect to the terms of this Agreement as if each of them had been a party hereto as an Author. The Author warrants that the use, reproduction, distribution, public or private performance or display, and/or modification of all or any portion of the Materials does not and will not violate, infringe and/or misappropriate the patent, trademark, intellectual property or other rights of any third party. The Author represents and warrants that it has and will continue to comply with all government, institutional and other regulations, including, without limitation all institutional, laboratory, hospital, ethical, human and animal treatment, privacy, and all other rules, regulations, laws, procedures or guidelines, applicable to the Materials, and that all research involving human and animal subjects has been approved by the Author's relevant institutional review board.

10. JoVE Discretion. If the Author requests the assistance of JoVE in producing the Video in the Author's facility, the Author shall ensure that the presence of JoVE employees, agents or independent contractors is in accordance with the relevant regulations of the Author's institution. If more than one author is listed at the beginning of this Agreement, JoVE may, in its sole discretion, elect not take any action with respect to the Article until such time as it has received complete, executed Article and Video License Agreements from each such author. JoVE reserves the right, in its absolute and sole discretion and without giving any reason therefore, to accept or decline any work submitted to JoVE. JoVE and its employees, agents and independent contractors shall have

jove JOURNAL OF VISUALIZED EXPERIMENTS
1 Alewife Center #200
Cambridge, MA 02140
tel. 617.945.9051
www.jove.com

ARTICLE AND VIDEO LICENSE AGREEMENT

full, unfettered access to the facilities of the Author or of the Author's institution as necessary to make the Video, whether actually published or not. JoVE has sole discretion as to the method of making and publishing the Materials, including, without limitation, to all decisions regarding editing, lighting, filming, timing of publication, if any, length, quality, content and the like.

11. Indemnification. The Author agrees to indemnify JoVE and/or its successors and assigns from and against any and all claims, costs, and expenses, including attorney's fees, arising out of any breach of any warranty or other representations contained herein. The Author further agrees to indemnify and hold harmless JoVE from and against any and all claims, costs, and expenses, including attorney's fees, resulting from the breach by the Author of any representation or warranty contained herein or from allegations or instances of violation of intellectual property rights, damage to the Author's or the Author's institution's facilities, fraud, libel, defamation, research, equipment, experiments, property damage, personal injury, violations of institutional, laboratory, hospital, ethical, human and animal treatment, privacy or other rules, regulations, laws, procedures or guidelines, liabilities and other losses or damages related in any way to the submission of work to JoVE, making of videos by JoVE, or publication in *JoVE* or elsewhere by JoVE. The Author shall be responsible for, and shall hold JoVE harmless from, damages caused by lack of sterilization, lack of cleanliness or by contamination due to the making of a video by JoVE its employees, agents or independent contractors. All sterilization, cleanliness or decontamination procedures shall be solely the responsibility of the Author and shall be undertaken at the Author's expense. All indemnifications provided herein shall include JoVE's attorney's fees and costs related to said losses or damages. Such indemnification and holding harmless shall include such losses or damages incurred by, or in connection with, acts or omissions of JoVE, its employees, agents or independent contractors.

12. Fees. To cover the cost incurred for publication, JoVE must receive payment before production and publication the Materials. Payment is due in 21 days of invoice. Should the Materials not be published due to an editorial or production decision, these funds will be returned to the Author. Withdrawal by the Author of any submitted Materials after final peer review approval will result in a US$1,200 fee to cover pre-production expenses incurred by JoVE. If payment is not received by the completion of filming, production and publication of the Materials will be suspended until payment is received.

13. Transfer, Governing Law. This Agreement may be assigned by JoVE and shall inure to the benefits of any of JoVE's successors and assignees. This Agreement shall be governed and construed by the internal laws of the Commonwealth of Massachusetts without giving effect to any conflict of law provision thereunder. This Agreement may be executed in counterparts, each of which shall be deemed an original, but all of which together shall be deemed to me one and the same agreement. A signed copy of this Agreement delivered by facsimile, e-mail or other means of electronic transmission shall be deemed to have the same legal effect as delivery of an original signed copy of this Agreement.

A signed copy of this document must be sent with all new submissions. Only one Agreement required per submission.

CORRESPONDING AUTHOR:

Name:	Delphine Gomez
Department:	Department of Medicine, Division of Cardiology
Institution:	University of Pittsburgh
Article Title:	Quantitative analysis of cellular composition in atherosclerotic lesions of smooth muscle cell lineage-tracing mice
Signature:	
Date:	02/21/18

Please submit a signed and dated copy of this license by one of the following three methods:

1) Upload a scanned copy of the document as a pfd on the JoVE submission site;
2) Fax the document to +1.866.381.2236;
3) Mail the document to JoVE / Attn: JoVE Editorial / 1 Alewife Center #200 / Cambridge, MA 02139

For questions, please email submissions@jove.com or call +1.617.945.9051

Response to the reviewer and editorial comments - JoVE59139

We want to thank the Reviewers for the constructive comments and suggestions for revisions. We feel that we have addressed virtually all of the reviewers' points and that the revised manuscript is much improved. For ease of review, our responses are in blue.

Reviewer #1:

Manuscript Summary:

Mahan et. al. described a standard protocol to characterize the cellular composition of murine atherosclerotic lesions with paraffin-embedded sections, immunofluorescent staining and confocal microscopy with focus on the brachiocephalic arteries. The effect of Interleukin-1β inhibition on SMC phenotype is shown as an example.

Major Concerns:

Figure 4C is not clear and rather confusing, should be removed.

We thank the reviewer for this comment and agree on the lack of clarity of Figure 4. Other reviewers raised a concern about the broad application of our single-cell counting method that we initially performed using the Nikon NIS-Elements software and possible inter-software variations. To address this concern, we have modified our protocol and described single-cell counting and phenotyping using ImageJ. Key parameter setting and representative pictures of single cell counting using ImageJ are included in Figure 5.

Minor Concerns:

Smooth muscle cell lineage-tracing mouse diet and treatment:

- Temperature of PBS and PFA solutions for perfusion should be indicated

PBS and 4% PFA solutions are used at room temperature. We added this information in the text.

- Source of high fat diet should be indicated

We indicated the source (vendor, catalog number) of high-fat and chow diet in the Materials list associated with the manuscript.

Harvesting the Brachiocephalic artery

- In the protocol point #5 "Exposing the BCA." BCA abbreviation used should be indicated before in the text.

We modified the text accordingly. We defined BCA the title of section 2: “Harvesting of the Brachiocephalic Artery (BCA).”

- Protocol point #6 "Removing the BCA" Reference to figure 2C does not correspond to the figure 2C but to figure2B.

We have modified Figure 2 and changed the references to Figure 2 subpanels accordingly.

Tissue Processing and sectioning

- The use of foam pads in the cassette to ensure the tissues retain correct orientation and remain in the cassette is difficult to imagine, to overcome this point a real picture of an embedding cassette with the artery should be included. In addition, a short description of the type and source of the embedding cassette used.

We added a picture of the BCA and right carotid artery positioned in the cassette and added cassettes (Figure 3) and foam pads to the Materials list.

- For how long where the cassettes immersed in 70% ethanol should be mentioned

Cassettes are immersed in 70% ethanol solution for 24 to 72 hours. Cassettes remain in 70% ethanol solution until tissues processing. Although the time of immersion in 70% ethanol solution can vary based on laboratory or histology core facility schedules, we did not experience variation in immunofluorescent staining for the incubation times mentioned above.

- Reference of Figure 2D on the text does not correspond with figure

We have modified Figure 2 and changed the references to Figure 2 subpanels accordingly.

- Description and source of microtome blade used should be included

The reference of the microtome blades was added to the Materials list.

- Reference of Figure 2E on the text does not correspond with figure

We have modified Figure 2 and changed the references to Figure 2 subpanels accordingly.

Immunofluorescence staining

- Point #4, temperature to incubate the slides in PBS for 5 min should be indicated

All incubations in PBS are performed at room temperature. We added the information in the text.

Representative results

Figure 2A

- "and Apoe-/- mouse fed a high fat diet for 26 weeks (right picture)" must be revised. Figure 2A right actually shows a 26-week-old Apoe-/- fed an 18 weeks high fat diet.

We revised Figure 2A (now Figure 2C) accordingly.

Figure 4

- Figure 4A: A proper delineation of the atherosclerotic lesion image is not shown and should be including.

We agree with the reviewer that the delineation of the regions selected for single-cell counting is critical. We decided to present in Figure 4 representative images illustrating how delineation of the lesion and fibrous cap areas are performed. We also included delineation of the areas of interest for single cell counting on each representative image in Figures 6 and 7.

- Figure 4B: Figure legend does not correspond to actual figure and labels

- Figure 4C: not essential for the methodology of this manuscript.

We have modified the content of the figures, and we hope that the Reviewer will find that these revised versions provide more clarity to illustrate key steps of single cell counting (Figures 4 and 5) and examples of staining and counting of the fibrous cap area (Figure 6) and lesion area (Figure 7).

Discussion

- Conclusion and other sentences such as: "This method allows for a meticulous assessment of lesion morphology and cellular composition" should be revised since the method described here does not provided steps to evaluate lesion morphology which includes lumen diameter but only provide a standard protocol to characterize the cellular composition as stated in the tittle.

We agree with the Reviewer that although we routinely perform lesion morphology analysis based on Movat staining, our manuscript does not describe this protocol and focus on immunofluorescent staining based single cell counting. Consequently, we have carefully edited the discussion and removed any mention to lesion morphometric analysis.

Reviewer #2:

Manuscript Summary:

This manuscript describes a protocol to standardize the evaluation of advanced atherosclerotic lesions in the brachiocephalic artery of ApoE-deficient lineage-tracing mice. The standardized analysis of advanced plaques, in particular their cellular composition, could provide important information for future intervention studies. There are several issues that should be addressed by the authors.

Major Concerns:

1. A major problem is the low quality of the IF pictures shown in Figs. 3 and 4, making it impossible to evaluate the immunofluorescence data. In Fig. 3, the DAPI staining is not visible at all. Please provide higher resolution images for Figs. 3 and 4. In addition, show a better DAPI staining in Fig. 3 and scale bars in Fig. 4.

We are sorry for the lack of quality of the pictures presented in the initial version of the manuscript. We carefully edited the figures, and we used images with a minimal resolution of 300 dpi. Based on the reviewer comment, we also change the color of DAPI staining from blue to gray to increase the visibility. We added scale bars to all images (Figure 4, 6 and 7) except for representative images in Figure 5. These pictures are screen captures illustrating the key parameter setting and single cell counting using ImageJ. We also systematically added the delineation of the region subjected to single cell counting (i.e., fibrous cap area in Figure 6, and lesion area in Figure 7).

2. Fig. 3 and Fig. 4: Compared to the staining of RUNX2 and YFP, the LGALS3 staining pattern looks very much different. Where are these proteins localized in the cells? Are the respective IF-positive structures single cells? It is sometimes difficult to match DAPI and IF signal. How was the specificity of the antibodies validated? How reliable is single-cell counting performed by the image software (line 328)? Have authors validated automatic counting by comparing with manual counting?

We thank the Reviewer for these pertinent questions:

1. RUNX2 is a transcription factor localized in the nucleus. YFP and LGALS3 are located in the cytoplasm.

2. Manual single cell counting allows the assessment of the association of cytoplasmic staining like YFP and LGALS3 with single nuclei (DAPI). We increase the brightness of DAPI for clarity.

3. Every staining is validated by the used of an isotype-matched IgG control. Confocal settings are based on the IgG control picture to assure that non-specific signal, if any, is excluded from the acquisition.

4. All single cell counting data presented in the manuscript has been acquired by manual counting. We have not, thus far, found automated software to perform cell counting reliably.

5. For broader applicability of our protocol and manuscript, we have replaced the use of a brand-specific microscope software by ImageJ, free software provided by the NIH. Of note, cell counting is still performed manually. ImageJ is used to visualize images and perform manual population annotations.

3. It appears that some of the IF pictures contain "black boxes" that cover distinct parts of the IF stainings, e.g. in Fig. 3 upper row (IgG control) "LGALS3" or in Fig. 4B, "3. YFP+ counting". Please explain why.

The pictures do not include any black box, modification, or alteration. We are sorry that the low quality of the picture or a mistake during the figure preparation leads the reviewer to this impression. We modify the figures to include high quality (300 to 600 dpi) images. We are happy to provide raw images upon request.

4. It should be indicated that injection of tamoxifen and high fat feeding are animal experiments and require approval of animal protocols. Moreover, tamoxifen is a biohazard and must be handled with care.

We have modified the manuscript accordingly.

5. Lineage tracing should be explained in more detail. Please describe the used mouse lines (correct names with references) and how the experimental animals were generated by breeding and identified by genotyping.

We extended the description of the lineage tracing system and the breeding strategy used to generate the experimental mice. We provided the reference of the three strains obtained from Jackson Laboratory and used to generate the atheroprone SMC lineage tracing mice (*Myh11* cre/ERT2^{+} *R26R*-EYFP$^{+/+}$ ApoE$^{-/-}$). We and others employed the generic strain names used in previous studies and listed as official nomenclature by Jackson Laboratory (mouse provider).

6. Authors make a strong point about the importance of perfusing the mouse with a "gravity perfusion system" that mimics physiological blood pressure (120/70 mmHg). Please explain how this pressure can be achieved.

We added a schematic of the gravity-driven perfusion station that we use in our laboratory and the equation to determine the pressure of perfusion (Figure 2).

The pressure is driven by the height of the column of liquid independently of the shape, total mass, or surface area of the liquid. The pressure is calculated as followed:

$P = \rho \times g \times h$ with:

P: Pressure in kg/ms^2 or Pascal (Pa) 1 mmHg = 133.322 Pa

ρ: Density of fluid in kg/m^3. The density of 4% PFA solution in PBS is 1016.8 kg/m^3

g: Acceleration of Gravity in m/s^2 = 9.8 m/s^2

h: Height of fluid in m.

With our system, the height of the fluid varies between h_1 = 1.5 m and h_2 = 1.35 m

Thus, the pressure of perfusion is comprised between:

P_1 = 1016.8 * 9.8 * 1.5 = 14946.96 Pa = 112.11 mmHg and,

P_2 = 1016.8 * 9.8 * 1.35 = 13452.264 Pa = 100.9 mmHg

In Figure 3, we included this equation and indicated the heights to reach the average systolic blood pressure in mice (120 mmHg).

We also mentioned in the text that a perfusion pump can also control the pressure of perfusion. It allows a finer control and consistency in the perfusion pressure. However, this option is certainly more expensive and maybe less broadly available to in contrast with the gravity perfusion system that can be built by investigators.

7. It is understand able that authors cite their own work on lineage tracing (e.g. refs 13 in line 110; refs 15/16 in line 112 and line 426). However, they should present a more balanced introduction and discussion of the topic and also acknowledge the many other laboratories that have developed and used inducible lineage tracing of SMCs in atherosclerosis. In fact, this technique has been described already at the beginning of the 2000s.

We revised the fourth paragraph of the introduction to not only more precisely describe how SMC lineage tracing works but also acknowledge studies that have been used SMC lineage tracing systems. We mentioned seminal studies by Speer et al. utilizing SM22 Cre LacZ mice to identify SMC transdifferentiating into chondrogenic cells [1]. However, we also highlighted the major limitations of non-inducible Cre systems. We also cited more exhaustive studies employing inducible SMC-specific Cre (Myh11 [2-5]; Acta2 [2, 6]) and other types of reporters (mTmG [2], Confetti or rainbow mice [3-6], and LacZ [7]).

Please discuss the following issues in the section on "limitations of the methodology presented here" (beginning at line 466):

8. The analysis of a single vessel per mouse (brachiocephalic artery) might not be sufficient to get a realistic picture and should be combined with the analysis of additional atherosclerotic regions such as the aortic arch and abdominal bifurcations of the aorta. Similar results in different regions of the aorta should strengthen the relevance of the study. Also, considering the 3Rs principle of animal experimentation, it would be welcome to obtain as many data as possible per mouse.

We thank the reviewer for this pertinent comment. While the present protocol focuses on brachiocephalic artery analysis, similar studies can be done on other vascular beds using the same standardized procedures. Additional vessels of tissues of interest can be harvested at the same time (aortic root, aortic arch, abdominal aorta). Analysis of the aortic root region has been the focus of previous publications [8] including a JOVE manuscript [9]. We revised the discussion of the manuscript to include a discussion on the reviewer's concern.

9. Feeding ApoE-deficient mice a high fat diet for 26 weeks (18 weeks plus additional 8 weeks with/without intervention) will typically cause extensive atherosclerosis with large lesions and almost closed vessels or even death of the animals. In this model it will be difficult to detect pro-atherosclerotic effects of genetic or pharmacological interventions.

We respectfully disagree with the reviewer regarding the relevance of long-term intervention studies. We feel that a model in which the therapeutic intervention is performed on advanced atherosclerotic lesions recapitulates therapeutic interventions in patients with coronary artery disease. Indeed, atherosclerosis is an asymptomatic and silent disease in its first stage, and patients often experience symptoms with advanced atherosclerotic lesions. Besides, the mortality rate in mice between 18 and 26 weeks of high-fat diet does not exceed 5%. Using this experimental design, we were able to identify key modifications of atherosclerotic lesions after treatment with an anti-IL-1β antibody that are classically described as indices of plaque rupture.

That said, by no mean, we suggest that the protocol described in our manuscript can only be used for long-term intervention studies. The standardized tissue processing, sectioning, staining, and analysis described here can be implemented for virtually all types of atherosclerosis studies (short and long-term, prevention and intervention). We included a statement reflecting this point in the discussion.

10. Authors mention in the introduction (line 99-100) and discussion (line 436-437) that en face staining is unable to distinguish between fatty streaks and advanced lesion. It is, however, not clear how the present protocol can achieve this, if only advanced lesions are being analysed.

Once again, we give as an example the implementation of a standardized protocol for atherosclerotic tissue harvesting, processing, sectioning, staining, and analysis using our recent study consisting in long-term high fat diet associated with a pharmacological intervention. This analysis of atherosclerotic vessel cross-section by immunofluorescent staining allows a rigorous investigation of the lesion size (based on DIC images; see figure 4) and cell composition and the determination of the stage of atherosclerotic lesions (fatty streaks vs. advanced lesions). In contrast, *en face* Sudan IV staining, while informative regarding atherosclerosis burden, cannot be used to assess the disease stage, lesion morphology, or cell composition.

11. The Myh11CreERT2 transgene is integrated on the Y chromosome, so only male mice can be studied.

This is correct; the *Myh11* Cre/ERT2 transgene is located on the Y chromosome precluding the use of female mice for these studies. This is a limitation for sex difference studies that we added to the list of limitations detailed in the last paragraph of the discussion. However, this is to date the most rigorous and reliable SMC lineage tracing system.

Minor Concerns:

12. Line 3: Revise title: "…composition in ADVANCED atherosclerotic lesions of…

We agreed with this suggestion and modified the title accordingly.

13. Line 133: How is the Tam solution prepared?

The description of tamoxifen preparation has been added.

14. Line 199: Fig. 2C should red Fig. 2B

15. Line 225: Fig. 2D should read Fig 2C

16. Line 238: Fig. 2E should read Fig 2D

We fixed Figure 2 and its reference in the text.

17. Line 246-248: "Lesion morphology, collagen content, and intraplaque hemorrhage can be analyzed by Movat, PicroSirius Red, Ter119 staining, respectively." Please include references to aid readers finding the corresponding protocols.

References were added to the section mentioned above.

18. Line 305: Give an example for "mounting media suitable for fluorescence".

Reference of the mounting media is listed in the Materials List associated with the manuscript.

Reviewer #3:

Manuscript Summary:

This manuscript details a procedure for systematic characterization of morphology, and cell populations present in brachiocephalic arteries in murine models of atherosclerosis. The proposed protocol is intended to standardize assessment of lesions specifically in an intervention setting, but would also be applicable to prevention studies. This is a useful framework for anyone working in pre-clinical atherosclerosis models.

Major Concerns:

-Delineating fibrous cap area and/or necrotic core is an extremely important and non-trivial step in quantifying such sections. Please describe exactly how one would differentiate fibrous cap and necrotic core from the rest of the lesion.

We agree with the reviewer that delineation of the lesion or sub-compartments of the lesions (i.e., fibrous cap, necrotic core) should be standardized to accurately compare the effects of two experimental conditions on the cellular composition and distribution. We added in the manuscript the description and representative images (Figure 4) of the delineation of the lesion and the fibrous cap area based on z-stack confocal images and published papers [10, 11].

- It is probably important to quantitate staining for various cell populations at some regular interval over the course of the whole BCA. Please suggest what you believe to be the optimum number of sections, and interval between them, that should be assessed.

We thank the reviewer for this important remark. The standardized protocol that we present here allows the unambiguous analysis by IF staining at precise locations along the brachiocephalic artery. For cell composition analysis by IF staining, we suggest to stain and analyze the lesions at two distances from the aortic arch. We suggest in the manuscript to analyze sections at 480 μm and 780 μm from the aortic arch. Additional locations can be investigated, but there should be consistency in the number of sections and their locations.

We included in the revised version of the manuscript an example of single cell counting at two different locations of cell populations within the fibrous cap area (Figure 6).

Minor Concerns:

- Good fixation is not indicated by livery discoloration. Liver discoloration indicates sufficient removal of blood, but does not necessarily indicate proper fixation.

We agree with the reviewer. We removed the inaccurate sentence from the text.

- Gravity-driven perfusion does not guarantee constant flow speed and pressure. It is highly prone to variability due to bubbles in the lines, user error when it comes to placement of the needle in the heart, duration of time the mouse is in the CO2 (i.e. quality of the heart to pump the fluid through the circulation), etc. Perhaps describe how you set up your system such that you achieve 70-120mmHg pressure.

Although the use of a gravity perfusion system does not guarantee a lack of variation of flow speed and pressure of PBS or PFA solutions, by far this method permits a much higher consistency than manual syringe perfusion. Also, perfusion of PBS and PFA solutions at a pressure close to physiological blood pressure avoids major alteration of the vessel and atherosclerotic lesion morphology. As indicated in the protocol, bubbles in the tubing system are flushed out before insertion of the needle into the apex of the left ventricle. All parameters including the time of euthanasia into the CO2 chamber, the location of insertion of the needle in the apex of the left ventricle, the volume of solutions perfused are kept as consistent as possible. We added in Figure 2 a schematic of the gravity perfusion system. We also included calculation of the height range for the gravity perfusion system based on the hydrostatic pressure equation: Pressure = density of fluid * acceleration of gravity * height.

- Line 227: I don't know what you mean by "face the blocks." Do you mean section the blocks?

Facing a block consists in removing the top section of the block where there is only paraffin, but not the tissue. Once sections include the tissue, they should be collected for careful assessment of the location and orientation. We rephrased the sentence in the manuscript.

- line 239: perhaps explain why less than or more than 10um sections would not be desirable.

Unlike thinner sections, 10 μm thick sections allow the quantification and unambiguous characterization of a larger number of cells. The acquisition of 8 to 10 μm thickness by stacks of 1 μm using a confocal microscope permits to associate a given staining (e.g., YFP, ACTA2, and LGALS3) to a single nucleus more accurately. Assessing the colocalization of the lineage tracing reporter and other phenotypic markers with single nuclei along several consecutive stacks is critical to avoid inaccuracy due to the proximity of several cells. This point has already been discussed [12, 13] and justify the use of 10 μm-thick sections and z-stack confocal microscopy.

- Line 268: perhaps list how many watts that ends up being in your microwave?

For antigen retrieval treatment in the microwave, we set up the machine at 50% power. Considering that our microwave has a maximal power of 1350W, the wattage during the antigen retrieval incubation is 675. Higher wattage can be used, but it will require optimization of the time of incubation.

- The description of single-cell counting seems fairly specific to your software. Hopefully the video associated with this manuscript will show how this is done in such a way that it is

generalizeable across software platforms. Is there open-source software that could be used for this?

We thank the reviewer for this highly pertinent comment and the great idea to adapt the protocol to open-source software. We elected to develop a single cell counting protocol using Image J, NIH supplied free software. The text has been modified accordingly, and Figure 5 illustrates the key steps of the procedure using Image J as well as representative pictures of counting.

- The figures seem to be in a low-quality format and the IFs are difficult to see in the reviewer version. I cannot see the annotations in figure 4.

We apologize for the low quality of the figures in the previous version of the manuscript. We increase the quality of the images.

Reviewer #4:

Manuscript Summary:

The manuscript describes a protocol for quantification of smooth muscle cell-derived cells in atherosclerotic lesions using genetic lineage tracing. Detailed protocols covering the entire experiment from genetic labelling, diet, dissection, tissue processing to immunostaining, imaging and quantification are included. While protocols for individual steps are readily available elsewhere, this presents a comprehensive collection that would be very useful to newcomers to the field. However, the protocol is very biased as detailed below, which limits it's quality. This could be accounted for by discussing alternative analyses.

Major comments:

Atherosclerotic lesions are very heterogeneous and the region considered for quantification has immense impact on the result. In the present manuscript this is very poorly described (line 330: " Delineate the region to analyze "). It is crucial that this delineation is more clearly described: how are the regions selected for quantification, and how are the appropriate regions identified in a confocal image (ie w/o H&E staining - even if this is provided for an adjacent section).

We thank the Reviewer for this comment highlighting the lack of information in the initial version of our manuscript.

First, we agree with the reviewer that if possible, the analysis should not be limited to one vascular bed and that vascular territory-specific differences can appear after pharmacological or genetic interventions. We focused on analyzing the cell composition and the SMC phenotype in the brachiocephalic artery, but similar analyses can be done on cross-sections of the aortic sinus or abdominal aorta. We mentioned this point in the discussion section of the revised manuscript.

Second, we provided more details regarding the delineation of regions of interest, namely the lesion area and the fibrous cap area, based on confocal images (see new Figure 3). We use Differential Interference Image (DIC) to localize precisely the intima and the internal elastic lamina. We trace along these borders to delimit the lesion area. The fibrous cap is classically defined the accumulation of Acta2+ cells and extracellular matrix components (including collagen) under the endothelial layer. Previous studies have shown that the average thickness of the fibrous cap in Apoe-/- mice fed with a WD for 18 to 26 weeks was 30 µm [10, 11, 14]. However, as highlighted by the Reviewer, plaques may not have a fibrous cap with a constant thickness or a continuous coverage of the endothelial layer. That said, we believe that the detailed analysis of the cellular composition in the 30µm-thick area localized under the endothelial layer (30µm fibrous cap area) is an objective and unbiased method to ascertain the changes in this critical region. The combination of DIC and ACTA2 channels allows measuring the 30 µm thick area under the intima. Examples of delineation of the lesion and the fibrous cap areas are shown in Figure 3.

The protocol describes analysis of lesions in the BCA of Myh11-CreERt2/EYFP/ApoE-null animals using FFPE, which appears unjustly restricted. In my opinion this should be corrected. For example,

* The advantages and disadvantages of FFPE are discussed, but it would be beneficial to mention alternatives - such as analysis of frozen samples to allow for direct detection of fluorescent protein expression, eliminating potential issues with antibody specificity

* Atherosclerosis development in different vascular beds appear to be differentially controlled (e.g. Newman et al JCI insight 2018), hence the focus on a single vascular bed might obscure important effects

* Other reporters have been used successfully for smooth muscle cell lineage tracing

We agreed with the reviewer and mentioned that similar immunofluorescence analysis of frozen sections in the discussion section. This protocol focuses on the analysis of BCA lesions by immunofluorescent staining on PFFE tissue sections. By no mean, this analysis excludes the use of alternative tissues, vascular beds and the implementation of complementary techniques. We have developed further this point in the discussion section.

Other lineage-tracing strategies have been reported including the use of alternative inducible Cre [1, 2, 6], and labeling (tomato/GFP [2], rainbow or confetti for clonal expansion analysis [3-6]). We have expanded the introduction section on SMC lineage tracing to reflect these alternatives as well as to mention the first generation of lineage tracing systems used in the 2000's by Speer et al. [1]. However, we emphasize that an inducible system be necessary for rigorous tracing of the SMC. Indeed, a caveat of the use of lineage tracing models employing non-inducible Cre systems, such as the widely used SM22 Cre LacZ is that any cell not coming originally from the SMC lineage would be positive for the tracing system upon activation of the SMC marker gene.

The manuscript includes data on how IL1beta neutralising antibody treatment affect Runx2 expression in the plaque. This data is derived from animals used for a recently published study

(Gomez et al Nat Med 2018). This point is not a concern - however, the data collection (region of analysis, number of cells quantified etc) is poorly described and the data is only compared for all cells. The conclusions made appears to be based on very preliminary analysis and in my opinion this data should not be included.

We think that it provides an example of analysis that can be performed with this protocol. However, we agree with the reviewer that the description of the quantification parameters was missing. In the new version of the manuscript, we provided two examples of single cell counting in the fibrous cap area (Figure 6) or the lesion area (Figure 7). We have provided more detail about these analyses in the representative results sections.

Minor comments:

References to figure 2 are wrong

We have modified Figure 2 and revised the references in the text.

The genotype annotation (line 131: Myh11 ERt2 Cre YFP Apoe-/-, sometimes R26R is used with YFP) is unconventional.

We revised the manuscript to employ consistent genotype annotations: Myh11 Cre/ERT2 and R26R eYFP. These annotations have been used before and are listed as official nomenclature by Jackson Laboratory.

Tissue processing conditions:

* Appear to lack an ethanol gradient - is this a typo?

We thank the reviewer for noticing our mistake. We corrected the tissue processing protocol.

* Conditions appear harsh (length of incubation times) for mouse BCA, with the risk of drying out the tissue and introducing artifacts

We corrected the tissue processing protocol. We routinely use this protocol, and we have not found that it introduces artifacts or alterations of the tissue.

* It would be worth mentioning that Xylene can be substituted with other clarifying agents that are more friendly to the environment and the operator (e.g. Histoclear)

Although we agree that environment-friendly reagents should be suggested when possible, we have reservations stating in the article that Histoclear is a good substitute to Xylene since we have never tested and compared the use of Xylene and Histoclear.

Details lacking:

Details of the tamoxifen solution makeup to ensure bioavailability should be included (line 154)

Tamoxifen is dissolved in preheated peanut oil and incubated at 55 °C on a rotator until the full dissolution of Tamoxifen. A more detailed protocol has been included in the revised version of the manuscript.

Reference for EDTA vacuum tube needed (line 155)

The reference and catalog number of the EDTA vacuum tube have been added to the Materials list associated with the manuscript.

Editorial comments:

Changes to be made by the author(s) regarding the manuscript:

1. Please take this opportunity to thoroughly proofread the manuscript to ensure that there are no spelling or grammar issues.

The manuscript was carefully proofread.

2. Please define all abbreviations before use.

All abbreviations are defined before use.

3. Please include an ethics statement before your numbered protocol steps, indicating that the protocol follows the animal care guidelines of your institution.

We added the ethics statement.

4. Please adjust the numbering of the Protocol to follow the JoVE Instructions for Authors. For example, 1 should be followed by 1.1 and then 1.1.1 and 1.1.2 if necessary. Please refrain from using bullets, dashes, or indentations.

We edited the manuscript accordingly.

5. Please revise the protocol text to avoid the use of any personal pronouns (e.g., "we", "you", "our" etc.).

We edited the manuscript accordingly.

6. Please revise the protocol to contain only action items that direct the reader to do something (e.g., “Do this,” “Ensure that,” etc.). The actions should be described in the imperative tense in complete sentences wherever possible. Avoid usage of phrases such as “could be,” “should be,” and “would be” throughout the Protocol. Any text that cannot be written in the imperative tense may be added as a “Note.” Please include all safety procedures and use of hoods, etc. However, notes should be used sparingly and actions should be described in the imperative tense wherever possible. Please move the discussion about the protocol to the Discussion.

7. Please revise the Protocol steps so that individual steps contain only 2-3 actions per step and a maximum of 4 sentences per step. Use sub-steps as necessary.

We edited the manuscript accordingly.

8. Please add more details to your protocol steps. There should be enough detail in each step to supplement the actions seen in the video so that viewers can easily replicate the protocol.

Please ensure you answer the “how” question, i.e., how is the step performed? Alternatively, add references to published material specifying how to perform the protocol action. See examples below.

We edited the manuscript accordingly.

9. Line 154: Please describe how to perform cardiac puncture. What volume of blood is collected?

We provided a more detailed description of the cardiac puncture.

10. Line 157: What is used to withdraw the top plasma phase?

Pipette and tips. We edited the manuscript accordingly.

11. Lines 162-167: Please specify all surgical instruments used. How large is the incision?

The incision is made with scissors and is approximatively ~ 2cm large. We edited the manuscript accordingly.

12. Lines 179: How large is the incision?

The incision is approximatively ~ 2mm large. We edited the manuscript accordingly.

13. Line 259: What does diH2O refer to?

diH2O refers to deionized H2O. The abbreviation is now defined after its first use.

14. Line 262: Please add more specific details (or move the details in lines 263-271 to the actual step).

We edited the manuscript accordingly.

15. Line 284: Please specify incubation temperature.

We edited the manuscript accordingly.

16. Line 315-316: Please provide specific values (ranges).

We edited the manuscript accordingly.

17. Lines 330-337: Software steps must be more explicitly explained ('click', 'select', etc.). Please add more specific details (e.g. button clicks for software actions, numerical values for settings, etc.) to your protocol steps.

We edited the manuscript accordingly.

18. Please include single-line spaces between all paragraphs, headings, steps, etc.

We edited the manuscript accordingly.

19. After you have made all the recommended changes to your protocol (listed above), please highlight 2.75 pages or less of the Protocol (including headings and spacing) that identifies the essential steps of the protocol for the video, i.e., the steps that should be visualized to tell the most cohesive story of the Protocol.

We highlighted the steps that should be included in the video.

20. Please highlight complete sentences (not parts of sentences). Please ensure that the highlighted part of the step includes at least one action that is written in imperative tense. Please do not highlight any steps describing anesthetization and euthanasia.

Done.

21. Please include all relevant details that are required to perform the step in the highlighting. For example: If step 2.5 is highlighted for filming and the details of how to perform the step are given in steps 2.5.1 and 2.5.2, then the sub-steps where the details are provided must be highlighted.

Done.

22. Please remove commercial language and use generic terms instead: Shandon Excelsior, Eppendorf, etc.

We edited the manuscript accordingly.

23. Figure 2D: Please include a space between all numbers and their corresponding units (i.e., 10 µm, 130 µm, 280 µm, etc.).

We edited the figures accordingly.

24. Figure 3: Please also explain the DAPI and Merge images in the figure legend.

We edited the figure legends accordingly.

25. Figure 5: Please define error bars in the figure legend.

Results are expressed as mean ± SEM. We added this information in figure legends.

26. References: Please do not abbreviate journal titles.

We used the JoVE style output in Endnote for citation and bibliography formatting.

REFERENCES

1. Speer, M.Y., et al., *Smooth muscle cells give rise to osteochondrogenic precursors and chondrocytes in calcifying arteries.* Circ Res, 2009. **104**(6): p. 733-41.
2. Herring, B.P., et al., *Previously differentiated medial vascular smooth muscle cells contribute to neointima formation following vascular injury.* Vasc Cell, 2014. **6**: p. 21.
3. Chappell, J., et al., *Extensive Proliferation of a Subset of Differentiated, yet Plastic, Medial Vascular Smooth Muscle Cells Contributes to Neointimal Formation in Mouse Injury and Atherosclerosis Models.* Circ Res, 2016. **119**(12): p. 1313-1323.
4. Dobnikar, L., et al., *Disease-relevant transcriptional signatures identified in individual smooth muscle cells from healthy mouse vessels.* Nat Commun, 2018. **9**(1): p. 4567.
5. Misra, A., et al., *Integrin beta3 regulates clonality and fate of smooth muscle-derived atherosclerotic plaque cells.* Nat Commun, 2018. **9**(1): p. 2073.
6. Sheikh, A.Q., et al., *Smooth muscle cell progenitors are primed to muscularize in pulmonary hypertension.* Sci Transl Med, 2015. **7**(308): p. 308ra159.
7. Majesky, M.W., et al., *Differentiated Smooth Muscle Cells Generate a Subpopulation of Resident Vascular Progenitor Cells in the Adventitia Regulated by Klf4.* Circ Res, 2017. **120**(2): p. 296-311.
8. Daugherty, A., et al., *Recommendation on Design, Execution, and Reporting of Animal Atherosclerosis Studies: A Scientific Statement From the American Heart Association.* Circ Res, 2017. **121**(6): p. e53-e79.
9. Venegas-Pino, D.E., et al., *Quantitative analysis and characterization of atherosclerotic lesions in the murine aortic sinus.* J Vis Exp, 2013(82): p. 50933.
10. Gomez, D., et al., *Interleukin-1beta has atheroprotective effects in advanced atherosclerotic lesions of mice.* Nat Med, 2018. **24**(9): p. 1418-1429.
11. Shankman, L.S., et al., *KLF4-dependent phenotypic modulation of smooth muscle cells has a key role in atherosclerotic plaque pathogenesis.* Nat Med, 2015. **21**(6): p. 628-37.
12. Bennett, M.R., S. Sinha, and G.K. Owens, *Vascular Smooth Muscle Cells in Atherosclerosis.* Circ Res, 2016. **118**(4): p. 692-702.
13. Bentzon, J.F. and M.W. Majesky, *Lineage tracking of origin and fate of smooth muscle cells in atherosclerosis.* Cardiovasc Res, 2018. **114**(4): p. 492-500.
14. Alexander, M.R., et al., *Interleukin-1beta modulates smooth muscle cell phenotype to a distinct inflammatory state relative to PDGF-DD via NF-kappaB-dependent mechanisms.* Physiol Genomics, 2012. **44**(7): p. 417-29.

Response to editorial comments – Resubmission 2 - JoVE59139

We have modified the figures accordingly to the editor's requests.

Editorial comments:

1. Figure 2B: "Heigh" should be "Height".
   We modified Figure 2B accordingly.
2. Please remove 'Figure 1"/"Figure 2"/etc. from the Figures themselves; please remove unnecessary white space as well.
   We removed the title on each figure and the extra white space as requested.